Atmospheric Mercury Concentrations observed at ground-based monitoring sites globally distributed in the framework of the GMOS network

Francesca Sprovieri[1], Nicola Pirrone[2], Mariantonia Bencardino[1], Francesco D'Amore[1], Francesco Carbone[1], Sergio Cinnirella[1], Valentino Mannarino[1], Matthew Landis[3], Ralf Ebinghaus[9], Andreas Weigelt[9], Ernst-Günther Brunke[8], Casper Labuschagne[8], Lynwill Martin[8], John Munthe[14], Ingvar Wängberg[14], Paulo Artaxo[18], Fernando Morais[18], Henrique de Melo Jorge Barbosa[18], Joel Brito[18], Warren Cairns[15], Carlo Barbante[15,25], María del Carmen Diéguez[10], Patricia Elizabeth Garcia[10], Aurélien Dommergue[4,24], Helene Angot[4,24], Olivier Magand[24,4], Henrik Skov[20], Milena Horvat[17], Jože Kotnik[17], Katie Alana Read[6], Luis Mendes Neves[7], Bernd Manfred Gawlik[12], Fabrizio Sena[12], Nikolay Mashyanov[13], Vladimir Obolkin[23], Dennis Wip[16], Xin Bin Feng[19], Hui Zhang[19], Xuewu Fu[19], Ramesh Ramachandran[11], Daniel Cossa[22], Joël Knoery[5], Nicolas Marusczak[22], Michelle Nerentorp[21], and Claus Norstrom[20]

[1]CNR Institute of Atmospheric Pollution Research, Rende, Italy
[2]CNR Institute of Atmospheric Pollution Research, Rome, Italy
[3]US-EPA, Environmental Protection Agency, Office of Research and Development, RTP, NC,USA
[4]Univ. Grenoble Alpes, Laboratoire de Glaciologie et Géophysique de l'Environnement, Grenoble, France
[5]LBCM, Ifremer, - Centre Atlantique, Nantes, France
[6]NCAS, University of York, UK
[7]CapeVerde Observatory, INMG- São Vicente, Cape Verde
[8]Cape Point GAW Station, Climate and Environ. Research & Monitoring, South African Weather Service
[9]Helmholtz-Zentrum Geesthacht, Germany
[10]INIBIOMA-CONICET-UNComa, Bariloche, Argentina
[11]Institute for Ocean Management, Anna University, India
[12]Joint Research Centre, Italy
[13]St. Petersburg State University, Russia
[14]IVL, Swedish Environmental Research Inst. Ltd., Sweden
[15]University Ca' Foscari of Venice, Italy
[16]University of Suriname, Dep. of Physics, Suriname
[17]Jožef Stefan Institute, Lubliana, Slovenia
[18]Univ. of Sao Paulo, Sao Paulo, Brazil
[19]State Key Laboratory of Environmental Geochemistry, Inst. of Geochemistry, Chinese Academy of Sciences
[20]AarhusUniversity, Department of Environmental Science, Denmark
[21]Chalmers University of Technology
[22]LER/PAC, Ifremer,Centre Méditerranée, La Seyne sur Mer, France
[23]Limnological Institute SB RAS, Irkutsk, Russia
[24]CNRS, Laboratoire de Glaciologie et Géophysique de l'Environnement, Grenoble, France
[25]CNR Institute for the Dynamics of Environmental Processes, Venice, Italy

Correspondence to: Francesca Sprovieri (f.sprovieri@iia.cnr.it)

Abstract. Long-term monitoring data of ambient mercury (Hg) on a global scale to assess its emission, transport, atmospheric chemistry, and deposition processes is vital to understand the impact of Hg pollution on the environment. The Global Mercury Observation System (GMOS) project was funded by the European Commission (www.gmos.eu), and started in November 2010 with the overall goal to develop a coordinated global observing system to monitor Hg on a global scale, including a large network of ground-based monitoring stations, ad-hoc periodic oceanographic cruises and measurement flights in the lower and upper troposphere, as well as in the lower stratosphere. To date more than 40 ground-based monitoring sites constitute the global network covering many regions where little to no observational data were available before GMOS. This work presents atmospheric Hg concentrations recorded worldwide in the framework of the GMOS project (2010-2015), analyzing Hg measurement results in terms of temporal trends, seasonality and comparability within the network. Major findings highlighted in this paper include a clear gradient of Hg concentrations between the Northern and Southern Hemisphere, confirming that the gradient observed is mostly driven by local and regional sources, which can be anthropogenic, natural or a combination of both.

1 Introduction

Mercury (Hg) is found ubiquitously in the atmosphere and is known to deposit to ecosystems, where it can be taken up into food-webs and transformed to highly toxic species (i.e., methyl-Hg) which are detrimental to ecosystem and human health. A number of activities have been carried out since the late 1980s in developed countries within European and International Strategies and Programs (i.e., UNECE-CLRTAP, EU-Mercury Strategy; UNEP Governing Council) to elaborate possible mechanisms to reduce Hg emissions to the atmosphere from industrial facilities, trying to balance the increasing emissions in rapidly industrializing countries of the world (Pirrone et al., 2013, 2008, 2009; Pacyna et al., 2010). Hg displays complex speciation and chemistry in the atmosphere, which influences its transport and deposition on various spatial and temporal scales (Douglas et al., 2012; Goodsite et al., 2004, 2012; Lindberg et al., 2007; Soerensen et al., 2010a, b; Sprovieri et al., 2010b; Slemr et al., 2015). Most of Hg is observed in the atmosphere as Gaseous Elemental Mercury (GEM/Hg0), representing 90 to 99% of the total with a terrestrial background concentration of approximately 1.5-1.7 $ng\ m^{-3}$ in the Northern Hemisphere and, between 1.0 and 1.3 $ng\ m^{-3}$ in the Southern Hemisphere based on research studies published before GMOS (Lindberg et al., 2007; Sprovieri et al., 2010b). The results obtained from newly established GMOS ground-based sites show a background value in the Southern Hemisphere close to 1 $ng\ m^{-3}$ which is lower than that obtained in the past. Oxidized Hg species (Gaseous Oxidized Mercury or GOM) and Particulate Bound Mercury (PBM) contribute significantly to dry and wet deposition fluxes to terrestrial and aquatic receptors (Brooks et al., 2006; Goodsite et al., 2004, 2012; Hedgecock et al., 2006; Skov et al., 2006; Gencarelli et al., 2015; De Simone et al., 2015). Although in the past two decades a number of Hg monitoring sites have been established (in Europe, Canada, USA and Asia) as part of regional networks and/or European projects (i.e., MAMCS, MOE, MERCYMS) (Munthe et al., 2001, 2003; Wängberg et al., 2001, 2008; Pirrone et al., 2003; Steffen et al., 2008) the need to establish a global network to assess likely Southern-Northern Hemispheric gradients and long-term trends has long been considered always a high priority for policy and scientific purposes. The main reason is to make consistent and globally distributed Hg observations

available that can be used to validate regional and global scale models for assessing global patterns of Hg concentrations and deposition and re-emission fluxes. Therefore a coordinated global observational network for atmospheric Hg was established within the framework of the Global Mercury Observation System (GMOS) project (Seven Framework Program - FP7) in 2010. The aim of GMOS was to provide high-quality Hg datasets in the Northern and Southern Hemispheres for a comprehensive assessment of atmospheric Hg concentrations and their dependence on meteorology, long-range atmospheric transport and atmospheric emissions on a global scale (Sprovieri et al., 2013). This network was developed by integrating previously established ground-based atmospheric Hg monitoring stations with newly established GMOS sites in regions of the world where atmospheric Hg observational data was scarce, particularly in the Southern Hemisphere (Sprovieri et al., 2010b). The stations are located at both high altitude and sea level locations, as well as in climatically diverse regions. The measurements from these sites have been used to validate regional and global scale atmospheric Hg models in order to improve our understanding of global Hg transport, deposition and reemission, as well as to provide a contribution to future international policy development and implementation (Gencarelli et al., 2016; De Simone et al., 2016). The GMOS overarching objective to establish a global Hg monitoring network was achieved having in mind the need to assure high-quality observations in line with international QA/QC standards and to fill the gap in terms of spatial coverage of measurements in the Southern Hemisphere were data were lacking or not existing. One of the major outcomes of GMOS has been an interoperable e-infrastructure developed following the Group on Earth Observations (GEO) data sharing and interoperability principles which allows to provide support to UNEP for the implementation of the Minamata Convention (i.e., Art.22 to measure the effectiveness of measures). Within the GMOS network, Hg measurements were in fact carried out using high-quality techniques by harmonizing the GMOS measurement procedures with those already adopted at existing monitoring stations around the world. Standard Operating Procedures (SOPs) and a QA/QC system were established and implemented at all GMOS sites in order to assure full comparability of network observations. To ensure a fully integrated operation of the GMOS network, a centralized online system (termed GMOS Data Quality Management, G-DQM) was developed for the acquisition of atmospheric Hg data in near real-time and providing a harmonized QA/QC protocol. This novel system was developed for integrating data control and is based on a service-oriented approach that facilitates real-time adaptive monitoring procedures, which is essential for producing high-quality data (Cinnirella et al., 2014; D'Amore et al., 2015). GMOS activities are currently part of the GEO strategic plan (2016-2025) within the GEO Flagship on "Tracking Persistent Pollutants". The overall goal of this flagship is to support the development of GEOSS by fostering research and technological development on new advanced sensors for in-situ and satellite platforms, in order to lower the management costs of long-term monitoring programs and improve spatial coverage of observations. In this paper we present for the first time a complete global dataset of Hg concentrations at selected ground-based sites in the Southern and Northern Hemispheres and highlight its potential to support the validation of global scale atmospheric models for research and policy scenario analysis.

2 Experimental

2.1 GMOS Global Network

The GMOS network currently consists of 43 globally distributed monitoring stations located both at sea level (i.e., Mace Head, Ireland; Calhau, Cape Verde; Cape Point, South Africa; Amsterdam Island, southern Indian Ocean) and high altitude locations, such as the Everest-K2 Pyramid station (Nepal) at 5050 m a.s.l. and the Mt. Walinguan (China) station at 3816 m a.s.l., as well as in climatically diverse regions, including polar areas such as Villum Research Station (VRS), Station Nord (Greenland), Pallas (Finland), and in Antarctica, Dome Concordia and Dumont d'Urville stations. It is possible to browse the GMOS monitoring sites at the GMOS Monitoring Services web portal. The monitoring sites are classified as Master (M) and Secondary (S) with respect to the Hg measurement programs (Table 1). Master Stations perform speciated Hg measurements and collect precipitation samples for Hg analysis whereas the Secondary Stations perform only Total Gaseus Mercury (TGM)/GEM measurements and precipitation samples as well. Table 1 summarize key information about GMOS stations, such as: a) the location, elevation and type of monitoring stations; b) new sites (Master and/or Secondary) established as part of GMOS; and c) existing monitoring sites established by institutions that are part of European and International monitoring programs and managed by GMOS partners and GMOS external partners who have agreed to share their monitoring data and submit them to the central database following the interoperability principles and standards set in GEOSS (Group Earth Observation System of System). The GMOS objective of establishing a global Hg monitoring network was achieved always bearing in mind not only the necessity to provide intercomparable data worldwide but also to meet international standards of intercomparibility. In particular, GMOS attempt to comply with the data sharing principles set by the Group on Earth Observations (GEO) aiming to develop the GEOSS encompassing: "observation systems: which include ground-, air-, water- and space-based sensors, field surveys and citizen observatories. GEO works to coordinate the planning, sustainability and operation of these systems, aiming to maximize their added-value and use; and... information and processing systems: which include hardware and software tools needed for handling, processing and delivering data from the observation systems to provide information, knowledge, services and products." In 2010 the Executive Committee of GEO selected GMOS as a showcase for the workplan (2012-2015) to demonstrate how GEOSS can support Convention and Policies as well as pioneering activity in environmental monitoring using highly advanced e-infrastructure. More details about the sites can also be found at: www.gmos.eu.

Eleven monitoring stations managed by external partners are included within the global network sharing their data with the GMOS central database. These new associated stations follow the "Governance and Data Policy of the Global Mercury Observation System" guidelines established by GMOS (Pirrone, 2012).

From the start of GMOS a small number of monitoring sites have been relocated or have become recently operational, however, most of the sites have been fully operational for the entire project period, and remain active. These original core group stations consist of 27 monitoring sites. Their spatial coverage is better throughout the Northern Hemisphere with 17 operational monitoring stations, whereas there are 5 sites in the Tropical Zone [area between the Tropic of Cancer (+23°27') and the Tropic of Capricorn(-23°27')], and 5 sites in the Southern Hemisphere. The sites in the Southern Hemisphere include new Hg stations, such as the GMOS site in Bariloche (Patagonia, Argentina), the station in Kodaicanal (South-India), and the

Table 1. Atmospheric ground-based sites locations that are part of the GMOS network and general characteristics of the sites (i.e., code, Lat, Lon), and including the type of monitoring station in respect to the Hg measurements carried out as speciated (M) or not (S).
*M=Master, S= Secondary; ** These sites use Lumex, elsewhere Tekran; **In bold External GMOS partners**

Code	Site	Country	Elev (m asl)	Lat°	Lon°	GMOS Site*
AMS	Amsterdam Island	Terres Australes et Antarctiques Françaises	70	-37.79604	77.55095	M
BAR	Bariloche	Argentina	801	-41.128728	-71.420100	M
CAL	Calhau	Cape Verde	10	16.86402	-24.86730	S
CHE	**Cape Hedo**	**Japan**	**60**	**26.86430**	**128.25141**	**M**
CPT	Cape Point	South Africa	230	-34.353479	18.489830	S
CST	Celestún	Mexico	3	20.85838	-90.38309	S
CMA	Col Margherita	Italy	2545	46.36711	11.79341	S
DMC	Concordia Station	Antarctica	3220	-75.10170	123.34895	S
DDU	Dumont d'Urville	Antarctica	40	-66.66281	140.00292	S
EVK	Ev-K2	Nepal	5050	27.95861	86.81333	S
ISK	Iskrba	Slovenia	520	45.56122	14.85805	M
KOD	Kodaicanal	India	2333	10.23170	77.46524	M
LSM	La Seyne-sur Mer	France	10	43.106119	5.885250	S
LIS**	Listvyanka	Russia	670	51.84670	104.89300	S
LON	Longobucco	Italy	1379	39.39408	16.61348	M
MHD	Mace Head	Ireland	8	53.32661	-9.90442	S
MAN	Manaus	Brazil	110	-2.89056	-59.96975	M
MIN	Minamata	Japan	20	32.23056	130.40389	M
MAL	Mt. Ailao	China	2503	24.53791	101.03024	S/M
MBA	**Mt. Bachelor**	**WA, USA**	**2743**	**43.977516**	**-121.685968**	**M**
MCH	Mt. Changbai	China	741	42.40028	128.11250	M/S
MWA	Mt. Walinguan	China	3816	36.28667	100.89797	M
NIK**	Nieuw Nickerie	Suriname	1	5.95679	-57.03923	S
PAL	Pallas	Finland	340	68.00000	24.23972	S
RAO	Rao	Sweden	5	57.39384	11.91407	M
SIS	Sisal	Mexico	7	21.16356	-90.04679	S
VRS	Villum Research Station	Greenland	30	81.58033	-16.60961	S

site on the Amsterdam Island (Terres Australes et Antarctiques Françaises, TAAF) in the southern Indian Ocean, and two sites in Antarctica at the Italian-French Dome Concordia station and at the French site Dumont d'Urville .

3 Hg Measurements Methods

3.1 Field Operation

All GMOS secondary sites used the Tekran Continuous Mercury Vapor Analyzer, Model 2537A/B (Tekran Instruments Corp., Toronto, Ontario, Canada) with the exception of Listvyanka site (LIS), Russia and Nieuw Nikerie site (NIK), Suriname, which used a Lumex RA-915+ mercury analyser. This last provides direct continuous GEM concentrations in air flow without Hg collection on sorbent traps (Sholupov and Ganeyev, 1995; Sholupov et al., 2004). GMOS Master Sites used the Tekran Model 2537A/B mercury vapor analyzer coupled with their speciation system Model 1130 for GOM, and Model 1135 for particulate boundaries mercury ($PBM_{2.5}$) with fractions less than 2.5 μm in diameter to prevent large particles from depositing on the KCl-coated denuder ((Gustin et al., 2015)). The principle and operation of the Tekran Hg speciation system are described in (Landis et al., 2002). Data was captured using either personal computers or data loggers and were submitted to the GMOS Central database network (www.gmos.eu/sdi). During the implementation of the GMOS global network, harmonized Standard Operating Procedures (SOPs) as well as common Quality Assurance/Quality Control (QA/QC) protocols have been developed (Munthe et al., 2011; Brown et al., 2010a, b) according to measurement practices followed within existing European and American monitoring networks and based on the most recent literature (Brown et al., 2010b; Steffen et al., 2012; Gay et al., 2013). The GMOS SOPs were reviewed by both GMOS partners and external partners as experts in this issue and finally adopted within the GMOS network (Munthe et al., 2011). Full SOPs are available online (www.gmos.eu/sdi) and include sections on site selection, field operations, data management, field maintenance and reporting procedures. All monitoring sites strictly followed the GMOS SOPs to harmonize operations and ensure the comparability of all results obtained worldwide. At the GMOS Master sites the Hg analyzers were operated in conjunction with the Tekran 1130/1135 speciation units, and therefore the TGM/GEM data for these sites are explicitly referred to as GEM. GEM concentrations were also provided by the two secondary sites (LIS and NIK) which used the Lumex Hg analyser (see the Lumex measurements principle in paragraph 2.2.2). Regarding the TGM/GEM at the other GMOS Secondary sites, it has been discussed whether the Tekran 2537A/B instruments measure TGM = GEM + GOM or GEM only (Slemr et al., 2011, 2015), and considering that previous modeling studies and experimental measurements highlighted that particularly at remote/background monitoring sites the oxidized fraction of the TGM is less than 2% (Gustin et al., 2015), we consider the Tekran 2537A/B data to represent GEM. This is also in line with a study recently published by (Slemr et al., 2015) which reports a comparison of Hg concentrations at several GMOS sites in the Southern Hemisphere. Following the SOPs implemented at all GMOS sites, the Hg analyzers used at the secondary sites were operated without the speciation units but using the PTFE (Teflon) filters to protect the instrument from sea salt and other particles intrusion. (Slemr et al., 2015) assumed that the surface active GOM in the humid air of the marine boundary layer at several GMOS secondary sites, mostly located at the coastline, [i.e., Cape Point (South Africa), Cape Grim (Australia) as well as Sisal (Mexico), Nieuw Nikerie (Paramaribo), Calhau (Cape Verde) etc.] has been filtered out together with PM, partly by the sea salt particles loaded PTFE filter and partly on the walls of the inlet tubing. Consequently, they assumed that measurements at the secondary sites represent GEM only and are thus directly comparable to those at remote Master sites. On the other hand, the observations made by (Temme et al., 2003) at Troll (Antarctica) suggested that at the low temperature and humidity pre-

vailing at this site, GOM passed the inlet tubing and the PTFE filter, measuring thus TGM and not GEM. Taking into account these findings, (Slemr et al., 2015) calculated for the GMOS Master site on Amsterdam Island (AMS) a value of GOM less than 1% of TGM compared to the other Secondary sites in the Southern Hemisphere, including Troll, highlighting therefore a value which is insignificant when compared with the uncertainties discussed in the available peer-reviewed literature (Slemr et al., 2015). Since we compare results at various stations, in this work we have taken into account analysis of both systematic and random uncertainties associated with the measurements as well as published results of Tekran intercomparison exercises as reported and discussed elsewhere (Slemr et al. (2015) and references there in).

3.2 GEM Measurements Method

Amalgamation with gold is the principle method used to sample Hg0 for atmospheric measurements worldwide (Gustin et al., 2015). The most widely used automated instrument is the Tekran 2537A/B analyser (Tekran Instrument Corp., Ontario, Canada) which performs amalgamation on dual gold cartridges used alternately, and thermal desorption (at 500°C) to provide continuous GEM measurements. One trap is sampling while the other is heated releasing Hg0 into an inert carrier gas (usually ultra-high purity argon), quantification is by Cold Vapor Atomic Fluorescence Spectroscopy (CVAFS) at 253.7 nm (Landis et al., 2002). Concentrations are expressed in $ng\ m^{-3}$ at Standard Temperature and Pressure (STP, 273.15 K, 1013.25 hPa). The sampling interval is between 5 and 15 min based on location logistics and meteorological conditions. Taking into account the elevation of some monitoring sites in the network (i.e., Ev-K2CNR, Nepal (5050 m a.s.l.), M.Waliguan, China (3816 m a.s.l.) and Concordia Station (3220 m a.s.l.), the Tekran 2537A/B analysers have been operated with a 15-minute sample time resolution at a flow rate of 0.8 $l\ min^{-1}$. Following the SOPs the Tekran analysers perform also automatic internal permeation source calibrations every 71 hours, and the best estimate of the method detection limit is 0.1 $ng\ m^{-3}$ at a flow rate of 1 $l\ min^{-1}$. The alternative automated instrument to measure continuous GEM concentrations is the Lumex RA-915AM which is based on the use of differential atomic absorption spectrometry with direct Zeeman effect providing a detection limit lower than 1 $ng\ m^{-3}$ (Sholupov and Ganeyev, 1995; Sholupov et al., 2004). Comparison studies between the Tekran 2537 and the RA-915AM performed both during EN 15852 standard development showed good agreement of the monitoring data obtained with these systems (Brown et al., 2010b).

3.3 GEM/GOM/PBM Measurements Method

Speciated atmospheric Hg measurements were performed using the Tekran Hg speciation system units (Models 1130 and 1135) coupled to a Tekran 2537A/B analyzer. PBM and GOM concentrations are expressed in picograms per cubic meter ($pg\ m^{-3}$) at STP (273.15 K, 1013.25 hPa). At most GMOS sites, the speciation units were located on the rooftop of the station and connected to a Tekran 2537A/B analyzer through a heated PTFE line (50 °C, 10m in length). The sampling time resolution, due to some technical/location issues, was set equal to 5, 10 and 15 min for GEM (see Tables in supplementary material) and equal to 1, 2 and 3 hrs for GOM and PBM. Speciation measurements were performed following the GMOS SOPs and procedure as described elsewhere (Landis et al., 2002) using a size selective impactor inlet (2.5 μm cut-off aerodynamic diameter at 10 l

min^{-1}), a KCl-coated quartz annular denuder in the 1130 unit, and a quartz regenerable particulate filter (RPF) in the 1135 unit.

3.4 Quality Assurance and Quality Control Procedures

In terms of network data acquisition, QA/QC implementation procedures, and data management, the worldwide configuration of the GMOS network was a challenge for all scientists and site operators involved in GMOS. The traditional approaches to Hg monitoring QA/QC management that were primarily site specific and manually implemented, were no longer easily applicable or sustainable when applied to a global network with the number and size of data streams generated from the monitoring stations in near real- time. The G-DQM system was designed to automate the QA process making it available on the web with a user-friendly interface to manage all the QC steps from initial data transmission through final expert validation. From the user's point of view, G-DQM is a web-based application, developed using a software as a Service (SaaS)-based approach (D'Amore et al., 2015). G-DQM is part of the GMOS Cyber-Infrastructure (CI), which is a research environment that supports advanced data acquisition, storage, management, integration, mining and visualization, built on an IT infrastructure (Cinnirella et al., 2014; D'Amore et al., 2015).

4 Results and Discussion

4.1 GMOS Data Coverage and Consistency

Almost all GMOS stations provide near real-time raw data that are archived and managed by GMOS-CI. Figures 1 and 2, over the 2011-2015 period, and at some of the ongoing Secondary and Master GMOS Stations, show the elemental and speciated Hg raw data coverage, respectively. For each station the Coverage of raw data was generated considering the percentage of the real available raw data in respect to the total potential number of data points on monthly basis. During the first year of the project a number of sites were being established and/or equipped and not enough data was available to support broad network spatial analysis. In 2011 (at the effectively starting of the project) only four monitoring sites produced Hg measurements, and step by step, an increasing number of stations have been established and added to the network in 2012. Therefore, we evaluated the two years 2013 and 2014 due to major data coverage (%) of the observations. In fact, our statistical evaluations/calculations are related to this period for all the ground-based sites taken into account within the GMOS network in order to harmonize the discussion and compare the results worldwide.

4.2 Northern - Southern Hemispheric Gradients

A summary of descriptive statistics based on monthly and annual averages from all GMOS sites is presented in Table SM1 and Table SM2. The 2013 and 2014 annual mean concentrations of 1.55 and 1.51 $ng\ m^{-3}$, respectively for the sites located in the Northern Hemisphere were calculated by averaging the 13 site means for both years. Similar calculations were made for the Southern Hemisphere and the Tropics (see Table SM1 and Table SM2). Annual mean concentrations of 1.23 and 1.22 $ng\ m^{-3}$

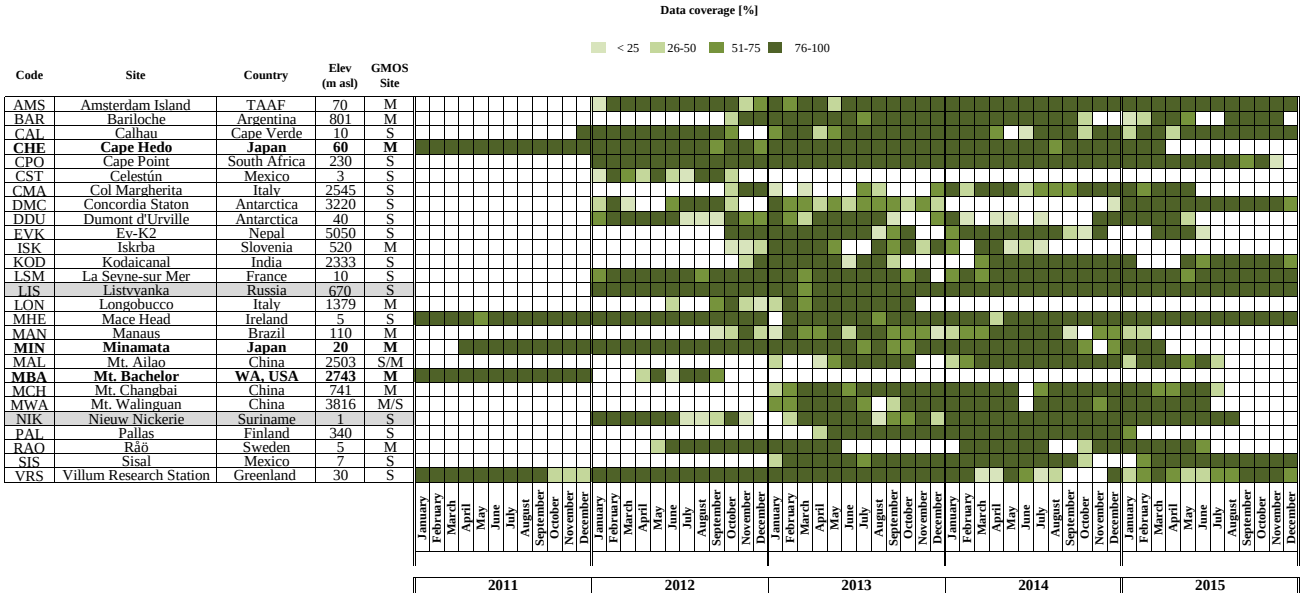

Figure 1. Coverage and consistency (%), on monthly basis, of GEM data collected at some of the on-going GMOS Secondary stations, over the period 2011-2015.

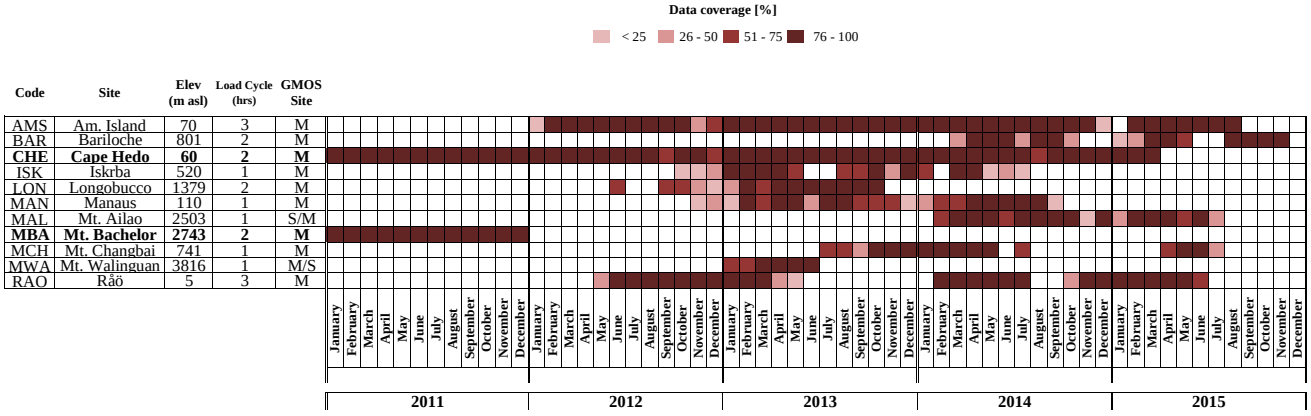

Figure 2. Coverage and consistency, on monthly basis, of GOM/PBM data collected at some of the on-going GMOS Master stations, over the period 2011-2015.

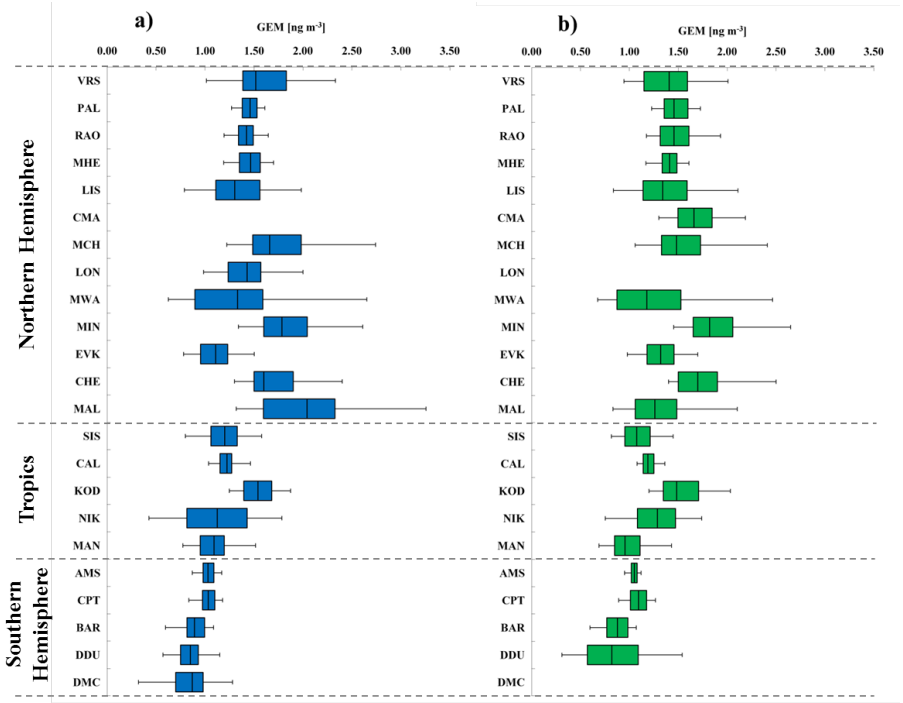

Figure 3. Box-and-whisker plots of gaseous elemental mercury yearly distribution (GEM, $ng\ m^{-3}$) at all GMOS stations for a) 2013 and b) 2014 years. The sites are organized according to their latitude from the Northern to the southern locations. Each box includes the median (midline), 25^{th} and 75^{th} percentiles (box edges), 5^{th} and 95^{th} percentiles (whiskers).

for 2013 and 2014, respectively were obtained in the Tropical zone, and 0.93 and 0.97 $ng\ m^{-3}$ for the Southern Hemisphere. Figure 3 shows the GEM yearly distribution for 2013 (blue) and 2014 (green). The sites have been organized in the graphic as well as in the Tables according to their latitude from those in the Northern Hemisphere, to those in the Tropics and in the Southern Hemisphere. The data so far does not cover a long enough time-span to investigate temporal trends, however some attempts have been previously made for the more established sites, such as Mace Head (MHD), Ireland (Ebinghaus et al., 2011; Weigelt et al., 2015), and Cape Point (CPT), South Africa (Slemr et al., 2015). At MHD the annual baseline GEM means observed by (Ebinghaus et al., 2011) decreased from 1.82 $ng\ m^{-3}$ at the start of the record in 1996 to 1.4 $ng\ m^{-3}$ in 2011 showing a downwards trend of 1.4-1.8% per year. Both a downward trend of 1.6% at MHD from 2013 and 2014 and the slight increase in Hg concentrations seen by (Slemr et al., 2015) at CPT from 2007 to 2013 continued throughout the end of 2014. Some debate remains as whether anthropogenic emissions are increasing or decreasing (Lindberg et al., 2002; Selin et al., 2008; Pirrone et al., 2013). A clear gradient of GEM concentrations between the Northern and Southern Hemispheres is seen in the data for both 2013 and 2014, in line with previous studies (Soerensen et al., 2010a, b; Sommar et al., 2010; Lindberg et al., 2007; Sprovieri et al., 2010b). The 13 northern sites had significantly higher median concentrations than did the southern sites. The north-south gradient is clearly evident in Figure 4 where are reported, respectively, the probability density functions

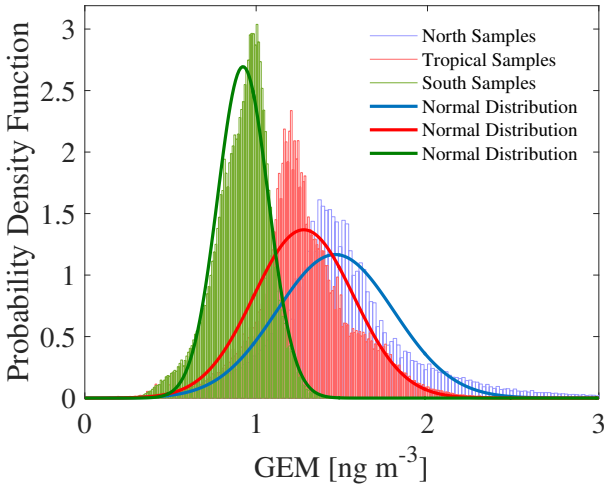

Figure 4. Probability density functions (PDFs) of the GEM data ($ng\ m^{-3}$) for the Northern, Southern and Tropical sample groups (dash dotted lines). Full lines the Normal distribution fit of the samples.

Table 2. The mean (X) of the experimental measures respectively for the Northern (X_N), Southern (X_S), and Tropical (X_T) groups, and the confidence intervals evaluated from the t-Student test among them.

Difference between means	Minimum of the confidence interval	Maximum of the confidence interval
$X_N - X_S$	0.590	0.592
$X_N - X_T$	0.225	0.229
$X_T - X_S$	0.362	0.365

(PDFs) of the data. The datasets have been divided into three principal groups related to the latitude: north samples, tropical samples and south samples, and the histograms, normalized to the unit area, has been constructed following the Scott rule for the bin width ΔW: $\Delta W = 3.5\sigma/\sqrt[3]{n}$, where σ represents the standard deviation and n the number of samples. This choice is optimal when deals with normal distributed samples since it minimizes the integrated mean squared error of the density estimate, then fitted trough a normal distribution (full line in Figure 4), obtained through the classical maximum likelihood estimation method. Since a clear overlap can be observed between the three data set presented in Figure 4, in order to make clear the distinction between the distributions we perform the standard t-Student test against the null hypothesis (h_0) that the three distributions come from the same mother distribution with the same mean (μ_0) and unknown standard deviation (σ_0). For every case the null hypothesis (h_0) can be rejected, say the means of the three distribution are significantly different, with a 99% confidence level. If X_N, X_S and X_T are the mean of the experimental measures respectively for the Northern, Southern and Tropical groups, the confidence intervals evaluated from the t-test are reported in Table 2. The interpretations of the results clearly demonstrate that $X_N > X_T > X_S$ (Table 2), so that there exist a significant gradient in the GEM concentrations from

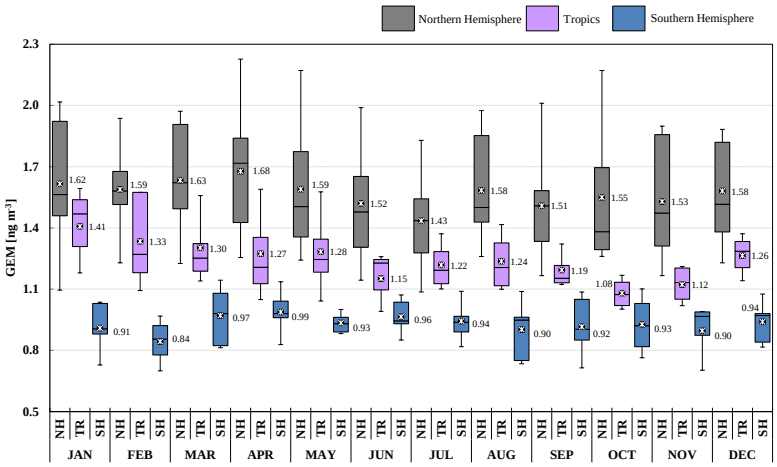

Figure 5. Monthly statistical distribution and spatial gradient for 2013 yr from Northern Hemisphere to Southern Hemisphere.

Northern Hemisphere to the Southern Hemisphere. Due to the significant difference in the PDFs, the probability p (p-value) of observing a test statistic as extreme as, or more extreme than, the observed value under the null hypothesis is close to zero. So that the validity of the null hypothesis should be rejected. The spatial gradient observed from north to south regions is also highlighted in both Figures 5 and 6 that also report the statistical monthly distribution of GEM values obtained for 2013 and 2014, respectively at all GMOS sites in the Northern and Southern Hemispheres as well as in the Tropical area.

4.2.1 Seasonal Patterns analysis in the Northern Hemisphere

Statistics describing the spatial and temporal distribution of GEM concentrations at all GMOS sites for 2013 and 2014 are summarized in Figure 3 whereas Figures 5 and 6 show the monthly statistical GEM distribution for both years considered. The GEM concentrations highlight that the mean GEM values of most of the GMOS sites were between 1.3 and 1.6 $ng\ m^{-3}$, with a typical interquartile range of about 0.25 $ng\ m^{-3}$. Only a few sites have shown a mean values above 1.6 $ng\ m^{-3}$, such as MCH, MIN, and MAL, and only the EVK site, located at 5050 m a.s.l. in the eastern Himalaya Mountains of Nepal, reported mean values below 1.3 $ng\ m^{-3}$. This value is comparable with free tropospheric concentrations measured in August 2013 over Europe (Weigelt et al., 2016). The mean GEM concentration observed at EVK is less than the reported background GEM concentration for the northern hemisphere (1.5-1.7 $ng\ m^{-3}$) and more similar to expected background levels of GEM in the Southern Hemisphere (1.1-1.3 $ng\ m^{-3}$) (Lindberg et al., 2007; Pirrone, 2016). The values between 1.3 and 1.6 $ng\ m^{-3}$ observed at the other GMOS sites in the Northern Hemisphere are comparable to the concentrations measured at the long-term

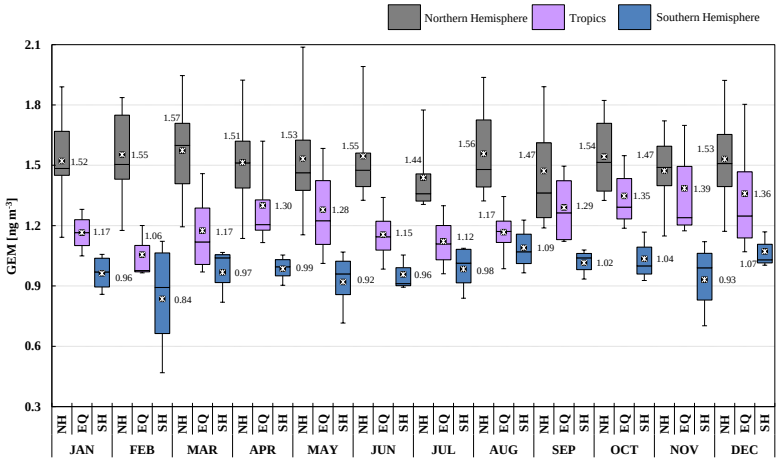

Figure 6. Monthly statistical distribution and spatial gradient for 2014 from Northern Hemisphere to Southern Hemisphere.

monitoring stations at Mace Head, Ireland (Ebinghaus et al., 2011; Slemr et al., 2011; Weigelt et al., 2015) and Zingst, Germany Kock et al. (2005). GEM concentration means are also in good agreement with the overall mean concentrations observed at multiple sites in the Canadian Atmospheric Mercury Measurement Network (CAMNet) (1.58 $ng\ m^{-3}$) reported by (Temme et al., 2007) and those reported from Arctic stations in this paper (VRS, PAL). Seasonal variations of GEM concentrations have been also observed at all GMOS sites in the Northern Hemisphere. Most sites show higher concentrations during the winter and spring, and lower concentrations in summer and fall seasons (Figures 5 and 6). However, few sites such as VRS, Station Nord (north-eastern Greenland, 81°36' N, 16°40'W) show a slightly different seasonal variation. In winter this High Arctic site (VRS) is sporadically impacted by episodic transport of pollution mainly due to high atmospheric pressure systems over Siberia and low pressure systems over the North Atlantic (Skov et al., 2004; Nguyen et al., 2013). During the spring (April-May) and summer (August-September) seasons GEM concentrations show a higher variability with low concentrations near the instrumental detection limit due to episodic atmospheric Hg depletion events (AMDEs) that occur in the Spring (Skov et al., 2004; Sprovieri et al., 2005a, b; Hedgecock et al., 2008; Steffen et al., 2008; Dommergue et al., 2010a), and high GEM concentrations (2 $ng\ m^{-3}$) in June and July, probably due to GEM emissions from snow and ice surfaces (Poulain et al., 2004; Sprovieri et al., 2005a, b, 2010b; Dommergue et al., 2010b; Douglas et al., 2012) and Hg evasion form the Arctic Ocean (Fisher et al., 2012; Dastoor and Durnford, 2014). Models of the Marine Boundary Layer (MBL) that simulate the temporal variations of Hg species (Hedgecock and Pirrone, 2005, 2004; Holmes et al., 2009; Soerensen et al., 2010b) show that photo-induced oxidation of GEM by Br can reproduce the diurnal variation of GOM observed in the MBL during cruise measurements better than other oxidation candidates (Hedgecock and Pirrone, 2005; Sprovieri et al., 2010a) and also the seasonal variation

(Soerensen et al., 2010b). Although Br is currently considered to be the globally most important oxidant for determining the lifetime of GEM in the atmosphere, there are also other possible candidates that can enhance Hg oxidation (Hynes et al., 2009; Ariya et al., 2008; Subir et al., 2011, 2012). The lack of a full understanding of the reaction kinetics and fate of atmospheric Hg highlights the need to have a global observation system as presented here in order to calibrate and constrain atmospheric box and global/regional scale models (Hedgecock and Pirrone, 2005; Dastoor et al., 2008).

4.2.2 GMOS Sites in Asia

As can be seen in Figure 3, the group with the highest GEM median variability and maximum concentrations is in Asia which include the following sites: Mt. Ailao (MAL), Mt. Changbai (MCH), Mt. Waliguan (MWA) and Minamata (MIN), where 95^{th}percentile values ranged from 3.26 to 2.74 $ng\ m^{-3}$ in 2013 (Table SM2). These sites are often impacted by air masses that have crossed emission source regions (AMAP/UNEP, 2013). GEM concentrations recorded at all remote Chinese sites (MAL, MCH, and MWA) are elevated compared to that observed at background/remote areas in Europe and North America, and at others sites in the Northern Hemisphere (Fu et al., 2012a, b, 2015). A previous study by (Fu et al., 2012a) at MWA suggested that long-range atmospheric transport of GEM from industrial and urbanized areas in north-western China and north-western India contributed significantly to the elevated GEM at MWA. MAL station is located in South-western China, at the summit of Ailao Mountain National Nature Reserve, in central Yunnan province. It is a remote station, isolated from industrial sources and populated regions in China. Kunming, one of the largest cities in South-western China, is located 180 km to the northeast of the MAL site. The winds are dominated by the Indian summer monsoon (ISM) in warm seasons (May to October), and the site is mainly impacted by Hg emission from eastern Yunnan, western Guizhou, and southern Sichuan of China and the northern part of the Indochinese Peninsula. In cold seasons the impact of emissions from India and north-western part of the Indochinese Peninsula increased and played an important role in elevated GEM observed at MAL (Zhang et al., 2015). However, most of the important Chinese anthropogenic sources of Hg and other air pollutants are located to the north and east of the station, whereas anthropogenic emissions from southern and western Yunnan province are fairly low (Wu et al., 2006; Kurokawa et al., 2013; Zhang et al., 2015). Average atmospheric GEM concentrations during this study calculated for MWA and MAL during 2013 and 2014 are in good agreement with those observed during previous measurements at both sites from October 2007 to September 2009 at MWA and from September 2011 to March 2013 at MAL (Fu et al., 2015; Zhang et al., 2015). Also the overall mean GEM concentration observed in 2013 and 2014 at MCH background air pollution site (1.66±0.48 $ng\ m^{-3}$, in 2013 and 1.48±0.42 $ng\ m^{-3}$, in 2014, respectively), is in good agreement with the overall mean value recorded earlier from 24 October 2008 to 31 October 2010 (1.60±0.51 $ng\ m^{-3}$, Fu et al., 2012).(Fu et al., 2012a) highlighted higher mean TGM concentration of 3.58±1.78 $ng\ m^{-3}$ observed from August 2005 to July 2006, probably due to surface winds circulation with effect of regional emission sources, such as large iron mining district in Northern part of North Korea and two large power plants and urban areas to the southwest of the sampling site. In summary, the observed concentrations are a function of site location relative to both natural and anthropogenic sources, elevation, and local conditions (i.e., meteorological parameters), often showing links to the patterns of regional air movements and long-range transport. Seasonal variations at ground-based remote sites in China have been observed. At MCH GEM was significantly higher during cold seasons compared to that

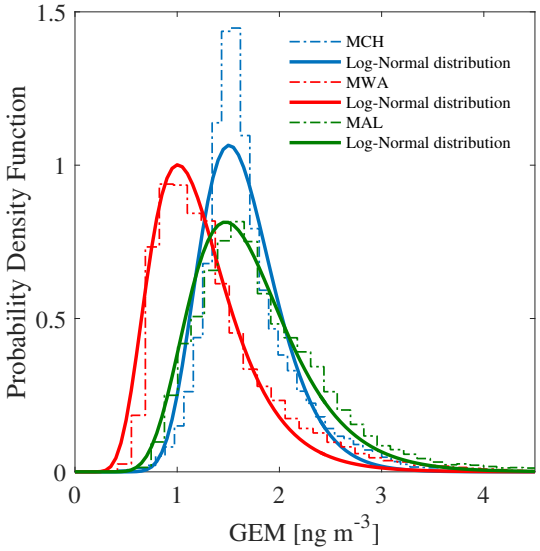

Figure 7. Probability density functions (PDFs) of the GEM data ($ng\ m^{-3}$) for the Chinese samples group (dash dotted lines). Full lines the Log-Normal distribution fit of the samples.

recorded in warm seasons (from April to September) whereas the reverse has been observed at the other two Chinese GMOS sites.

In order to statistically check the difference of GEM concentrations among the three Chinese sites an alternative statistical test has been performed, since in this case the distributions are strongly non-normal.

As in the previous case we construct the unit-area histogram, then we fit with a log-normal distribution. It is worth noting that in this case the histograms has been constructed by manually setting the bin width ΔW. With this choice the total number of bins can be evaluated as:

$$n = (X_{max} - X_{min})/\Delta W = 61$$

By looking at Figure 7, is easy to notice that the skewness ($\mu_3/\sigma^3 \sim 2$ where μ_3 is third order moment of the distribution and σ is the standard deviation) and the kurtosis ($\mu_4/\mu_2^2 \sim 10$ where μ_i is the i-th order moment of the distribution) are far from being zero. In the following the alternative is briefly described. Let us consider a pair of our three time series, namely X_i $(i = 1, 2)$ which corresponds to independent random samples described by the log-normal distributions. Then the random variables $Y_i = \ln(X_i)$ are close to normal distribution with means μ_i and variances σ_i^2, namely $Y_i \sim N(\mu_i, \sigma_i^2)$.

Since $\eta_i = \exp(\mu_i + 0.5\sigma_i^2)$ is the expectation value for X_i, the problem of our interest is then to test the null hypothesis about $\eta_2 - \eta_1$. More formally, we test $H_0 : \theta \leq 0$ where $\theta = \eta_2 - \eta_1$. In other words we test the null hypothesis that there is a significant difference in the sample means. Using the algorithm described in (Krishnamoorthya and Mathewb, 2003; Abdollahnezhad et al., 2012),specifically designed to perform the inference on difference of means of two log-normal distributions. We obtain the estimates for the p-values which are close to 1 and the confidence intervals, calculated at a confidence level of 95%, which

Table 3. Difference between the η_i obtained for MCH, MWA and MAL, confidence intervals and p-value associated.

Difference of η_i	Minimum of the confidence interval	Maximum of the confidence interval	P
$\eta_{MCH} - \eta_{MWA}$	0.285	0.286	1
$\eta_{MCH} - \eta_{MAL}$	0.043	0.043	1
$\eta_{MWA} - \eta_{MAL}$	0.328	0.329	1

are reported in Table 3. From the statistical results we can conclude that exist a clear distinction between the MWA site and the other two (MCH, MAL) as shown from the values in Table 3. However despite the large overlap in the samples distributions of MCH and MAL the difference in their η_i (η_{MCH} and η_{MAL} respectively) is also significant, with a smaller confidence interval.

Several hypothesis have been made to explain the seasonal variations of GEM in China, including seasonal changes in anthropogenic GEM emissions and natural emissions. The seasonal emission changes mainly resulted from coal combustion for urban and residential heating during cold seasons. This source lacks emission control devices and releases large amounts of Hg leading to elevated GEM concentrations in the area, and thus at MCH (Feng et al., 2004; Fu et al., 2008a, b, 2010). Conversely, GEM at MAL and MWA was higher in warm seasons than in cold seasons. These findings highlight that emissions from domestic heating during the winter could not explain the lower winter GEM concentrations observed at MWA and MAL but there might be other not-yet-understood factors that played a key role in the observed GEM seasonal variations at these sites, such as the monsoonal winds influence which can change the source-receptor relationship at observational sites and subsequently the seasonal GEM trends (An, 2000; Fu et al., 2015). Among the remote Chinese sites, MAL started as Secondary site and in 2014 was upgraded to a Master site; conversely, MWA started as Master site and then became a Secondary site whereas MCH operated continuously as Master site. Therefore, PBM and GOM concentrations have been measured during the years 2013 and 2014 at all Chinese sites even if not continuously (see Figure 2 for Hg speciation data coverage). The GOM and PBM concentrations measured at these sites were substantially elevated compared to the background values in the Northern Hemisphere, from 1.8 to 42.8 $pg\ m^{-3}$ and from 40.4 to 167.4 $pg\ m^{-3}$ at the MCH and MWA respectively, in 2013. The 2014 PBM maxima were 44.2 and 45.0 $pg\ m^{-3}$ at MCH and MAL, respectively. Regional anthropogenic emissions and long-range transport from domestic source regions are likely to be the primary causes of these elevated values (Sheu et al., 2013). Seasonal variations of PBM observed at the Chinese Master sites mostly showed lower concentrations in summer and higher concentrations (up to 1 order of magnitude higher) in winter and fall (Wang et al., 2006, 2007; Fu et al., 2008b; Zhu et al., 2014; Xu et al., 2015; Xiu et al., 2009; Zhang et al., 2013). The higher PBM in winter was likely caused by direct PBM emissions, formation of secondary particulate Hg via gas-particle partitioning and a lack of wet scavenging processes (Wang et al., 2006; Fu et al., 2008b; Zhu et al., 2014). PBM has an atmospheric residence time ranging from a few hours to several days and can therefore be transported to the remote sites when conditions are favourable (Sheu et al., 2013). Atmospheric particulate matter (PM) pollution is of special concern in China due to the spatial distribution of anthropogenic emissions concentrations of PM2.5 in heavily populated areas of eastern and northern China are among the highest in the world (van Donkelaar et al., 2010). The

GOM concentrations observed at both master sites show high variability and several episodes with high GOM values were probably due to local emission sources (such as domestic heating in small settlements) rather than to long-range transport from industrial and urbanized areas (Fu et al., 2015). GOM has a shorter atmospheric residence time that limits long-range transport (Lindberg and Stratton, 1998; Pirrone et al., 2008). However, with low RH and high winds, the possibility of regional transport of GOM cannot be ruled out. For example, the observations at MWA exhibit a number of high-GOM events related to air plumes originating from industrial and urbanized centres that are about 90 km east of the sampling site (Fu et al., 2012a; Pirrone, 2016). MWA is a remote site situated at the edge of the north-eastern part of the Qinghai-Xizang (Tibet) plateau. The monitoring station is relatively isolated from industrial point sources and there are no known local Hg sources around the site. Most of the Chinese industrial and populated regions associated with anthropogenic Hg emissions are situated to the east of MWA. Predominantly winds are from the west to southwest in cold seasons and the east in warm seasons (Pirrone, 2016). East Asia is, in fact, the largest Hg source region in the world, contributing to nearly 50% of the global anthropogenic Hg emissions to the atmosphere (Streets et al., 2005, 2011; Pirrone et al., 2010; Lin et al., 2010).

4.2.3 Seasonal Patterns analysis in the Southern Hemisphere

For the sites located in the Southern Hemisphere, the GEM concentrations highlight that the mean GEM values ranged between 0.84 and 1.09 $ng\ m^{-3}$, in both 2013 and 2014, with a typical interquartile range of about 0.25 $ng\ m^{-3}$ (see Figures 3, 5 and 6). The mean GEM concentrations observed at the southern sites are lower than those reported in the Northern Hemisphere but in good agreement with the southern hemispherical background (1.1 $ng\ m^{-3}$) (Lindberg et al., 2007; Sprovieri et al., 2010b; Lindberg et al., 2002; Dommergue et al., 2010b; Angot et al., 2014; Slemr et al., 2015; Soerensen et al., 2010a), and the expected range for remote sites in the Southern Hemisphere. As in the Northern Hemisphere, a seasonal variation of GEM concentrations was observed in the Southern Hemisphere. In particular, GEM concentrations from the coastal Global Atmosphere Watch station, Cape Point (CPT), South Africa show seasonal variations with maxima during austral winter and minima in summer. The site is located in a nature reserve at the southern-most tip of the Cape Peninsula on a hill, 230 m a.s.l. It is characterized by dry summers with moderate temperatures and increased precipitation (cold fronts) during austral winter. During the summer months, biomass burning events sometimes occur within the south-western Cape region affecting GEM levels. The dominant wind direction at CPT is from the southeastern sector advecting clean, maritime air from the South Atlantic Ocean (Brunke et al., 2004, 2012) which occur primarily during austral summer (December till February). Furthermore, the station is also at times subjected to air from the northern sector, mainly during austral winter. During such continental airflow events, anthropogenic emissions from the industrialized area in Gauteng, 1500 km to the north-east of CPT, can sometimes be observed (Brunke et al., 2012; Slemr et al., 2015). The GEM seasonal variability at CPT is hence in good agreement with the prevailing climatology at the site. Also GEM data at Amsterdam Island followed a similar trend, with slightly but significantly higher concentrations in winter (July-September) than in summer (December-February). Amsterdam Island is a remote and very small island of 55 km^2 with a population of about 30 residents, located in the southern Indian Ocean at 3400 km and 5000 km downwind from the nearest lands, Madagascar and South Africa, respectively (Angot et al., 2014). GEM concentrations at AMS were remarkably steady with an average hourly mean concentration of 1.03±0.08 ng

m^{-3} and a range of 0.72-1.55 $ng\ m^{-3}$. A small seasonal cycle has been observed by (Angot et al., 2014) and despite the remoteness of the island, wind sector analysis, air mass back trajectories and satellite observations suggest the presence of a long-range contribution from the southern African continent to the GEM regional/global budget from July to September during the biomass burning season extended from May to October (Angot et al., 2014). The higher GEM concentrations at AMS are comparable with those recorded at Calhau (Cape Verde), Nieuw Nickerie (Paramaribo), and Sisal (Mexico) in the Tropical zone, whereas the lower concentrations of GEM observed, less than 1 $ng\ m^{-3}$, were associated with air masses coming from southern Indian Ocean and the Antarctic continent. Bariloche (BAR) Master site in North Patagonia also shows higher concentrations during the austral winter (from end of May to September), and lower concentrations in other seasons (Diéguez et al., 2015). The Patagonian site has been established inside Nahuel Huapi National Park, a well-protected natural reserve, located at the east of the Patagonian Andes. The area is included in the Southern Volcanic Zone (SVZ) of the Andes, under the influence of at least three active volcanoes with high eruption frequency located at the west of the Andes cordillera, (Daga et al., 2014). The climate of the region is influenced by the year-round strong westerly winds blowing from the Pacific which discharge the humidity in a markedly seasonal way (fall-winter) in the western area of the Park. GEM records at BAR station show background concentrations comparable to that found in Antarctica and other remote locations of the South Hemisphere with concentrations ranging between 0.2 and 1.3 $ng\ m^{-3}$, with an annual mean of 0.89 ± 0.15 $ng\ m^{-3}$. Previous records of GEM concentrations from a short-term survey in 2007 along a longitudinal transect across the Andes with Bariloche as the eastern endpoint, reported concentrations below 2 $ng\ m^{-3}$ close to BAR (Higueras et al., 2014). In this survey, the highest GEM concentrations were recorded in the proximity and downwind from the volcanic area reaching concentrations up to 10 $ng\ m^{-3}$ (Higueras et al., 2014). Similarly to the seasonal trends at other GMOS sites in the Southern Hemisphere, GEM concentrations were at their lowest level in summer on the Antarctic Plateau at Concordia Station (DMC, altitude 3220 m) but at their highest level in fall (Angot et al., 2016b). GEM concentrations reached levels of 1.2 $ng\ m^{-3}$ from mid-February to May (fall) likely due to a low boundary layer oxidative capacity under low solar radiation limiting GEM oxidation, and/or a shallow boundary layer ($\sim$ 50 m in average) limiting the dilution. In summer (November to mid-February), the DMC GEM data showed a high variability with a concentration range varying from below the detection limit to levels comparable to those recorded at mid-latitude background Southern Hemisphere stations due to an intense chemical exchange at the air/snow interface. Additionally, the mean summertime GEM concentration at DMC was $\sim$ 25% lower than at other Antarctic stations in the same period of the year, suggesting a continuous oxidation of GEM as a result of the high oxidative capacity of the Antarctic plateau boundary layer in summer. GEM depletion events occurred each year in summer (January-February 2012 and 2013) with GEM concentrations remaining low ($\sim$ 0.40 $ng\ m^{-3}$) for several weeks. These depletion events did not resemble to the ones observed in the Arctic. They were not associated with depletion of ozone and occurred as air masses stagnated over the Plateau which could favor an accumulation of oxidants within the shallow boundary layer. These observations suggest that the inland atmospheric reservoir in Antarctica is depleted in GEM and enriched in GOM in summer. Measurements at DDU on the East Antarctic coast were dramatically influenced by air masses exported from the Antarctic Plateau by strong katabatic winds (Angot et al., 2016a). These results, along with observations from earlier studies, demonstrate that, in Antarctica, the inland atmospheric reservoir can influence the cycle of atmospheric Hg at a continental scale (Sprovieri et al., 2002; Temme et al.,

2003; Pfaffhuber et al., 2012; Angot et al., 2016b, a). Observations at DDU also highlighted that the Austral Ocean is a net source of GEM in summer and a net sink in spring, likely due to enhanced oxidation by halogens over sea-ice covered areas.

4.2.4 Seasonal Patterns Analysis in the Tropical Zone

Relatively few observations of atmospheric Hg had been carried out in the Tropics, before the start of GMOS. Until recently atmospheric Hg data for the tropics were only available from short term measurement campaigns. To date, therefore, there is no information in the Tropical area that can be used to establish long-term trends. Observations in this region may provide a valuable input to our understanding of key exchange processes that take place in the Hg cycle considering that the Inter Tropical Convergence Zone (ITCZ) passes twice each year over this region and the northern and southern hemispheric air masses may well influence the evolution of Hg concentrations observed in this region. As can be seen in Figure 3, five GMOS sites are located in the Tropics, including Sisal (SIS) in Mexico, Nieuw Nickerie (NIK) in Suriname, Manaus (MAN) in Brazil, Calhau (CAL) in Cape Verde and southern Kodaikanal (KOD) in southern India. GEM concentrations observed in 2013 and 2014 at all sites are comparable with Hg levels recorded at remote sites in the Southern Hemisphere (1.1 to 1.3 $ng\ m^{-3}$, Lindberg et al., 2007). Among these sites, the Kodaikanal site (KOD) shows the highest monthly mean GEM concentrations (see Figures 5 and 6 as well as Table SM1 and SM2) ranging between 1.25 $ng\ m^{-3}$ (5^{th}percentile) to 1.87 $ng\ m^{-3}$ (95^{th}percentile) during 2013 with an annually-based statistic mean of 1.54 ± 0.20 $ng\ m^{-3}$ and between 1.20 $ng\ m^{-3}$ (5^{th}percentile) to 2.03 $ng\ m^{-3}$ (95^{th}percentile) during 2014 with an annually average of 1.48 ± 0.26 $ng\ m^{-3}$ .KOD is a Global Atmospheric Watch (GAW) regional site which is operated by the Indian Meteorological Department. It is worth to point out that the other tropical GMOS sites are close to sea level and on the coast, whereas KOD is a high altitude site (2333 m a.s.l.). Therefore different meteo-climatic conditions influence the long range transport of air masses to this site. This site is also influenced by anthropogenic sources such as the well-known, but not close, Hg thermometer plant, 2150 m far away from the monitoring station at Kodaikainal (Karunasagar et al., 2006). Due to this anthropogenic influence atmospheric Hg concentrations from 3 $ng\ m^{-3}$ to 8 $ng\ m^{-3}$ for the years 2000 and 2001 have been reported (Rajgopal and Mascarenhas, 2006). India is the third largest hard coal producer in the world after the People's Republic China and the USA (Pirrone et al., 2010; Mason, 2009; Penney and Cronshaw, 2015). For the past three decades, India has increased the production of metals, cement, fertilizers and electricity through burning of coal, natural gas and oil becoming one of the most rapidly growing economies (Choi, 2003; Karunasagar et al., 2006). Relatively little attention has been paid to potential Hg pollution problems due to mining operations, metal smelting, energy and fuel consumption which could impact on ecosystem health (Mohan et al., 2012). Hg concentrations are in fact enhanced in India due to industrial emissions of Hg mostly from coal combustion (the major source category (48%), followed by waste disposal (31%), the iron and steel industry, chlor-alkali plants, the cement industry, and other minor sources (i.e., clinical thermometers) (Mukherjee et al., 2008; UNEP, 2008). Unfortunately, details of Hg emissions from these facilities and atmospheric Hg data in general are scarce. Therefore it is necessary for India as well as for the other place in the world where Hg measurement are yet lacking to generate continuous data, which can be used by scientists for modelling applications to improve emission inventories in order to prevent inaccurate assessments of Hg emission and deposition.

GEM levels observed at Sisal (SIS), Mexico, were below the expected global average concentration ($\sim 1.5 ng\ m^{-3}$). Monthly

mean GEM concentrations ranged between 1.0 to 1.47 $ng\ m^{-3}$ in 2013 with an annual average of 1.20 ± 0.24 $ng\ m^{-3}$ ($5^{th}$and 95^{th}percentile 0.8 and 1.58 $ng\ m^{-3}$), whereas in 2014 the range varied from 0.82 to 1.45 $ng\ m^{-3}$, with an annual average of 1.11 ± 0.37 $ng\ m^{-3}$ ($5^{th}$and 95^{th}percentile 0.82 and 1.45 $ng\ m^{-3}$). GEM measurements at SIS showed in addition, very little variability over the sampling period, indicating that this relatively remote site on the Yucatan Peninsula was not subject to any significant anthropogenic sources of Hg at all. During 2013 and 2014, the SIS site was typically influenced by the marine air originating from the Atlantic Ocean before entering the Gulf of Mexico (Sena et al., 2015). Average GEM concentrations reported at SIS are lower than those recorded in other rural places in Mexico, such as Puerto Angel (on the Pacific coast in Oaxaca state) and Huejutla (a rural area in the state of Hidalgo), where average values of 1.46 and 1.32 $ng\ m^{-3}$ were determined, respectively (de la Rosa et al., 2004). Low GEM concentrations were recorded in 2013 during the later part of the wet season (July/October). Those values may indicate a slight decrease probably due to deposition processes since the site is a coastal station and subject to frequent episodes with high humidity caused by rain (Sprovieri et al., 2016). These findings have also been confirmed through wind roses and backward trajectories that show the predominant wind direction from east-south-east most of the time and sometimes from east-north-east (Atlantic Ocean) (Sprovieri et al., 2016). In addition, the ITCZ moves north of the equator passing over the Yucatan peninsula during the northern hemisphere summer, causing tropical rain events which could contribute to the slight decrease of Hg concentrations. Highest GEM levels were observed during the winter period (Dec-Jan) in 2013, whereas 2014 had the lowest GEM concentration in January and higher GEM levels during spring and summer. The background Hg concentrations measured at Sisal are closely comparable to those recorded at Nieuw Nickerie (NIK), Paramaribo, Suriname, located on the north-eastern coast of the South American continent, the first long-term measurement site in the tropics which has been in operation since 2007 (Muller et al., 2012). Analysis of data shows that the annual mean GEM for 2013 and 2014 at NIK are a little lower than those at SIS, 1.13 ± 0.42 $ng\ m^{-3}$ and to 1.28 ± 0.46 $ng\ m^{-3}$, respectively (see Table SM1 and Table SM2). NIK is also a background site because most of the time the air masses arriving at the site come from the clean marine air of the Atlantic Ocean and the influence of possible local anthropogenic sources and continental air is minimal. As the ITCZ crosses Suriname twice each year, the NIK site samples both northern and southern hemispheric air masses. Occasionally higher values are seen, 1.57 $ng\ m^{-3}$ in Feb/Mar 2013 and 1.51 in Aug/Sep 2014 (see Figures SM1 and SM2). Manaus (MAN) in Amazonia (Brazil) is a GMOS Master site located in the Amazon region, an area with a history of important land use change and significant artisanal and small-scale gold mining activities since the 80s. Burning of natural vegetation to produce agriculture lands or pastures represents an important diffuse source of Hg to the atmosphere in Brazil (Lacerda et al., 2004; do Valle et al., 2005). The analysis of atmospheric Hg species at this site is thus important for the determination of the dynamics of atmospheric Hg. Annual mean Hg concentrations in 2013 and 2014 at MAN are slightly lower than those at both SIS and NIK, with little variability between the two years, see Table SM1 and Table SM2. The measurements from MAN station may therefore suggest that, although the Hg emissions from regional biomass burning and ASGM represent the major emission sources in the Amazon basin as reported in a study performed by (Artaxo et al., 2000), they may not have a significant impact locally, but contribute to the global Hg background (concerning Hg from biomass burning see (De Simone et al., 2015). Unfortunately the emissions from both these sources are associated with large uncertainties and vary over time. Quantifying their impact in South America is extremely important and there is a strong case

for expanding the number of GMOS measurements site in the region. MAN is in fact, a very remote site, inside the campus of the Embrapa Amazonia oriental and upwind from the three main gold mining areas in the Amazon basin which are located in Rondonia, Mato Grosso and in the South of the Parà states (Artaxo et al., 2000). Previous Hg measurements performed by (Artaxo et al., 2000) during an aircraft experiment over different sites in the Amazon Basin highlighted Hg concentrations between 0.5 to 2 $ng\ m^{-3}$ at pristine sites (and among them also MAN) not impacted by air-masses enriched with emissions from gold mining areas and/or biomass-burning. Those data collected from August to September, 1995 are comparable to ours observed in 2013 and 2014 at MAN during the same period, whereas at other sites over areas with intense biomass burning and near areas with strong Hg emissions (Alta Floresta and Rondonia, for example) reported very high Hg levels (5 - 14 $ng\ m^{-3}$)(Artaxo et al., 2000). These high Hg concentrations have never observed at MAN during the 2013 and 2014 period. Monthly mean GEM concentrations at MAN ranged in fact, between 1.01 to 1.18 $ng\ m^{-3}$ in 2013 and in 2014 between 0.94 to 1.10 $ng\ m^{-3}$. Also PBM and GOM recorded during 2013 show little variation and varied between 1.35 and 12.70 $pg\ m^{-3}$ ($5^{th}$and 95^{th}percentile, respectively) with a median value of 3.17 $pg\ m^{-3}$. In 2014, the range was from 0.53 to 5.24 $pg\ m^{-3}$ ($5^{th}$and 95^{th}percentile, respectively) with a median value of 1.48 $pg\ m^{-3}$. The MAN Hg concentrations therefore seem not to be influenced by regional emissions. However, a number of parameters, such as the intense air mass convection occurring in the Amazon basin and meteorological condition in general clearly contribute to the observed Hg concentrations, and they do not necessarily reflect only regional emissions (Artaxo et al., 2000; do Valle et al., 2005). Most of the air masses that reach the site in 2013 and 2014 comes from Tropical Atlantic, and travels for about 1,500 Km over pristine forest before reaching the site (Artaxo et al., 2015), and the prevailing winds during the wet seasons (from Jan-March) were from North-North-East, North-East, and East-North-East, whereas during the dry seasons (from Aug-Oct) were from North and North-North-East as well as North-North-West (Artaxo et al., 2015).

The Cape Verde Atmospheric Observatory, Calhau Station (CAL) contributes data from the Eastern tropical Atlantic Ocean, where GMOS provides the only existing data set. CAL is an important GAW station located on Sao Vicente Island, approximately 50m from the coastline. GEM measurements from 2012 to 2014 were broadly consistent with previously published oceanographic campaign measurements in the region, with typical Hg values between 1.1 and 1.4 $ng\ m^{-3}$. The prevailing wind was from the northeast open ocean bringing air masses from the tropical Atlantic and from the African continent (Mendes, 2014). Due to its relatively long residence time in the atmosphere, the ground level background GEM concentration tends to be relatively constant over the year in tropical regions, unlike mid-latitude and polar regions where a more noticeable seasonal variation has been observed. When compared with measurements from cruise campaigns from North to South Atlantic, we can see that the GEM data at CAL are similar to previously reported southern Atlantic data, where Hg concentrations are lower than the northern part of the Atlantic. Monthly mean GEM concentrations in 2013 ranged between 1.12 to 1.38 $ng\ m^{-3}$, with an annually-based mean of 1.22 ± 0.14 $ng\ m^{-3}$ ($5^{th}$and 95^{th}percentile equal to 1.04 $ng\ m^{-3}$ and to 1.46 $ng\ m^{-3}$, respectively), whereas in 2014, the monthly mean observed varied from 1.12 $ng\ m^{-3}$ to 1.33 $ng\ m^{-3}$ with an annually-based mean of 1.20 ± 0.09 $ng\ m^{-3}$($5^{th}$and 95^{th}percentile equal to 1.08 $ng\ m^{-3}$ and to 1.36 $ng\ m^{-3}$, respectively). The highest GEM concentrations in air originating from central Africa have been recorded at CAL when the relative humidity was lowest (occasionally during dust events) (Carpenter, 2011). All Tropical GMOS sites show little atmospheric Hg variability through both the years (2013

and 2014) with small GEM fluctuations during the months which well agrees with a relatively long atmospheric lifetime of Hg in the background troposphere and small variations in the source strength (Ebinghaus et al., 2002) however, clear diurnal cycles of Hg have been conversely observed.

5 Conclusions

The higher Hg concentrations and its spatio-temporal variability observed in the Northern Hemisphere compared to the Tropical area and Southern Hemisphere confirms that the majority of emissions and re-emissions are located in the Northern Hemisphere. The inter-hemispherical gradient with higher GEM concentrations in the Northern Hemisphere has remained nearly constant over the years, and confirmed by the observations carried out in the Southern Hemisphere and other locations where before GMOS Hg measurements were lacking or absent. Previous results on all cruises carried out over the oceans highlighted that in the Northern Hemisphere GEM mean values are almost generally higher than those obtained in the Southern Hemisphere, with a rather homogeneous distribution of GEM in the Southern Hemisphere. The stability of these background concentrations can be seen as evidence that the atmospheric lifetime of Hg is reasonably long to explain the extent of its dispersion, but would not be in accord with the most recent theoretical and experimental studies of the reaction rates of Hg with atmospheric oxidants. The oxidation of atmospheric Hg can occur with extraordinary rapidity, in the polar troposphere during the springtime Hg depletion events as well as within the marine boundary layer due to the reactions between Hg and bromine compounds although there are other possible reactants that can enhance Hg oxidation depending upon environmental factors and setting. These uncertainties highlight several Hg issue which have to be improved to better understand the atmospheric transport and transformation mechanisms of Hg. One concerns the chemical composition of the oxidised phase of atmospheric Hg, GOM and PBM, which are currently operationally defined but not still well understood. Field and laboratory studies highlighted analytical interferences within the methods currently adopted to measure oxidized Hg species which suggest the variation of the chemical compounds of them across space and time. This has significant implications for refining existing measurement methods and developing new techniques/methodologies capable of distinguishing between Hg compounds within different environmental compartments. Knowing the precise chemical composition of GOM would immediately provide impetus to those who study reaction kinetics to refine rate constants and reaction mechanisms as well as allow modeling studies chemical mechanisms to be verified improving our understanding of the important processes characterizing the atmospheric transport and transformation of Hg. The variation of observed Hg concentration across GMOS network shows increased amplitude in areas strongly influenced by anthropogenic sources. There are, however, uncertainties in the emission estimates especially for the tropical region and the Southern Hemisphere, and not enough long-term information in either areas to identify long-term trends. The lack of an advanced global emission inventory for regional and global scale models application represented another important objective of the GMOS network. In the last years several modeling studies have highlighted the discrepancy between modeled and observed concentrations of GEM at background sites primarily due to existing gaps on biomass burning, artisanal small scale gold mining and open coal bed fires contributions within the emission inventories for anthropogenic sources. Therefore, long-term atmospheric Hg measurements across the GMOS global network and additional

new GMOS ground-based sites increasingly incorporated into strategic areas are crucial to continue in the next future in order to provide high-quality measurement datasets which can give new insights and information about the worldwide trends of atmospheric Hg. The over-arching benefit of this coordinated Hg monitoring network would clearly be the advancement of the knowledge on Hg processes on global scale due to model/measurement comparisons, models development and validation on different spatial and temporal scales, and assessing trends with significant implications within the Task Force on Hemispheric Transport of Air Pollutants (HTAP-TF) in the context of a global model intercomparison aimed to study long-range transport pathways of pollutants and their precursors. The experience gained during GMOS, the development of SOPs for Hg monitoring and the establishment of the Spatial Data Infrastructure (SDI), http://www.gmos.eu/sdi/ (along GEOSS lines), which includes the G-DQM System provide a template to aid countries complying with the requirements of the Article 22 of the Minamata convention.

Acknowledgements. The number of people and institutions to acknowledge for their great contribution during field studies is quite significant for a project like GMOS, however we greatly acknowledge the European Commission for funding GMOS as part of the FP7 (contract no. 26511). Special thanks to those research scientists and technicians that helped to set up aircraft-based platform for UTLS measurements, ground-based sites in remote locations including EV-K2 in the Karakorum, Amsterdam Island, Dome C in Antarctica and all those involved in GMOstral 1028 (IPEV) project for field logistics and technical support.

References

Abdollahnezhad, K., Babanezhad, M., and Jafari, A. A.: Inference on Difference of Means of two Log-Normal Distributions; A Generalized Approach, Journal of Statistical and Econometric Methods, 1, 125–131, 2012.

AMAP/UNEP: Technical Background Report for the Global Mercury Assessment 2013, Tech. rep., Arctic Monitoring and Assessment Programme, Oslo, Norway/UNEP Chemicals Branch, Geneva, Switzerland, 2013.

An, Z.: The history and variability of the East Asian paleomonsoon climate, Quaternary Sci. Rev., 19, 171–187, doi:10.1016/S0277-3791(99)00060-8, 2000.

Angot, H., Barret, M., Magand, O., Ramonet, M., and Dommergue, A.: A 2-year record of atmospheric mercury species at a background Southern Hemisphere station on Amsterdam Island, Atmos. Chem. Phys., 14, 11 461–11 473, doi:10.5194/acp-14-11461-2014, 2014.

Angot, H., Dion, I., Vogel, N., Legrand, M., Magand, O., and Dommergue, A.: Multi-year record of atmospheric mercury at Dumont d'Urville, East Antarctic coast: continental outflow and oceanic influences, Atmospheric Chemistry and Physics, 16, 8265–8279, doi:10.5194/acp-16-8265-2016, http://www.atmos-chem-phys.net/16/8265/2016/, 2016a.

Angot, H., Magand, O., Helmig, D., Ricaud, P., Quennehen, B., Gallée, H., Del Guasta, M., Sprovieri, F., Pirrone, N., Savarino, J., and Dommergue, A.: New insights into the atmospheric mercury cycling in central Antarctica and implications on a continental scale, Atmospheric Chemistry and Physics, 16, 8249–8264, doi:10.5194/acp-16-8249-2016, http://www.atmos-chem-phys.net/16/8249/2016/, 2016b.

Ariya, P., Skov, H., Grage, M., and Goodsite, M.: Gaseous elemental mercury in the ambient atmosphere: review of the application of theoretical calculations and experimental studies for determination of reaction coefficients and mechanisms with halogens and other reactants, Adv. Quantum Chem., 55, 43–55, doi:10.1016/S0065-3276(07)00204-3, 2008.

Artaxo, P., de Campos, R., Fernandes, E., Martins, J., Xiao, Z., Lindqvist, O., Fernàndez-Jimènez, M., and W.Maenhaut: Large scale mercury and trace element measurements in the Amazon basin, Atmospheric Environment, 34, 4085–4096, 2000.

Artaxo, P., de Brito, J. F., Barbosa, H., Morais, F., Sprovieri, F., and Bencardino, M.: Mercury concentrations in Central Amazon Basin, http://www.gmos.eu/public/artaxo_poster_2015.pdf, 2015.

Brooks, S., Saiz-Lopez, A., Skov, H., Lindberg, S., Plane, J., and Goodsite, M.: The mass balance of mercury in the springtime arctic environment, Journal of Environmental Monitoring, 33, doi:10.1029/2005GL025525, 2006.

Brown, R., Pirrone, N., van Hoek, C., Horvat, M., Kotnik, J., Wängberg, I., Corns, W., Bieber, E., and Sprovieri, F.: Standardization of a European measurement method for the determination of total gaseous mercury: results of the field trial campaign and determination of a measurement uncertainty and working range, Accred. Qual. Assur., doi:10.1007/s00769-010-0636-2, 2010a.

Brown, R., Pirrone, N., van Hoek, C., Sprovieri, F., Fernandez, R., and Toté, K.: Standardisation of a European measurement method for the determination of mercury in deposition: results of the field trial campaign and determination of a measurement, Journal of Environmental Monitoring, 12, 689–695, doi:10.1039/b924955a, 2010b.

Brunke, E.-G., Labuschagne, C., Parker, B., Scheel, H., and Whittlestone, S.: Baseline air mass selection at Cape Point, South Africa: application of 222Rn and other filter criteria to CO2, Atmos. Environ., 38, 5693–5702, doi:10.1016/j.atmosenv.2004.04.024, 2004.

Brunke, E.-G., Ebinghaus, R., Kock, H., Labuschagne, C., and F. Slemr, S. A.: Emissions of mercury in southern Africa derived from long-term observations at Cape Point, Atmos. Environ., 12, 7465–7474, doi:10.5194/acp-12-7465-2012, 2012.

Carpenter: Seasonal characteristics of tropical marine boundary layer air measured at the Cape Verde Atmospheric Observatory, Journal of Atmospheric Chemistry, doi:10.1007/s10874-011-9206-1, 2011.

Choi, Y.: Recent development in India's IT industry and its implications. KIEP Publications, Seoul, Korea, IEEE Journal of Selected Topics in Applied Earth Observations and Remote Sensing, p. 73, 2003.

Cinnirella, S., D'Amore, F., Bencardino, M., Sprovieri, F., and Pirrone, N.: The GMOS cyber(e)-infrastructure: advanced services for supporting science and policy, Environmental Science and Pollution Research, 21, 4193–4208, doi:10.1007/s11356-013-2308-3, 2014.

Daga, R., Guevara, S., Poire, D., and Arribére, M.: Characterization of tephras dispersed by the recent eruptions of volcanoes Calbuco (1961), Chaitén (2008) and Cordón Caulle Complex (1960 and 2011), in Northern Patagonia, Journal of South American Earth Sciences, 49, 1–14, doi:10.1016/j.jsames.2013.10.006, 2014.

D'Amore, F., Bencardino, M., Cinnirella, S., Sprovieri, F., and Pirrone, N.: Data quality through a web-based QA/QC system: implementation for atmospheric mercury data from the Global Mercury Observation System, Environmental Sciences: Processes and Impacts, 17, 1482–1492, doi:10.1039/C5EM00205B, 2015.

Dastoor, A. and Durnford, D.: Arctic Ocean: Is it a sink or a source of atmospheric mercury?, Environ. Sci. Technol., 48, 1707–1717, 2014.

Dastoor, A., Davignon, D., Theys, N., Roozendael, M. V., Steffen, A., and Ariya, P.: Modeling dynamic exchange of gaseous elemental mercury at polar sunrise, Environ. Sci. Technol., 42, 1482–1492, doi:10.1021/es800291w, 2008.

de la Rosa, D., Volke-Sepulveda, T., Solarzano, G., Green, C., Tordon, R., and Beauchamp, S.: Survey of atmospheric total gaseous mercury in Mexico, Atmospheric Environment, 38, 4839 – 4846, 2004.

De Simone, F., Cinnirella, S., Gencarelli, C. N., Yang, X., Hedgecock, I. M., and Pirrone, N.: Model Study of Global Mercury Deposition from Biomass Burning, Environ. Sci. Technol., 49, 6712–6721, 2015.

De Simone, F., Cinnirella, S., Gencarelli, C. N., Carbone, F., Hedgecock, I. M., and Pirrone, N.: Particulate-Phase Mercury Emissions during Biomass Burning and Impact on Resulting Deposition: a Modelling Assessment, Atmospheric Chemistry and Physics Discussions, 2016, 1–22, doi:10.5194/acp-2016-685, http://www.atmos-chem-phys-discuss.net/acp-2016-685/, 2016.

Diéguez, M., García, P., and Sprovieri, F.: Atmospheric mercury fluxes in North Patagonia: first continuous records of the EMMA station (Global Mercury Observation System, Bariloche, Argentina), in proceedings ICMGP, 2015.

do Valle, C., Santana, G., Augusti, R., EgrejaFilho, F., and Windmoller, C.: Speciation and quantification of mercury in Oxisol, Ultisol, and Spodosol from Amazon (Manaus, Brazil), Chemosphere, 58, 779–792, 2005.

Dommergue, A., Larose, C., Fain, X., Clarisse, O., Foucher, D., Hintelmann, H., Schneider, D., and Ferrari, C.: Deposition of mercury species in the Ny-Alesund area (79 N) and their transfer during snowmelt, Environ. Sci. Technol., 44, 901–907, doi:10.1021/es902579m, 2010b, 2010a.

Dommergue, A., Sprovieri, F., Pirrone, N., Ebinghaus, R., Brooks, S., Courteaud, J., and Ferrari, C.: Overview of mercury measurements in the Antarctic troposphere, Atmospheric Chemistry and Physics, 10, 3309 – 3319, 2010b.

Douglas, T., Loseto, L., MacDonald, R., Outridge, P., Dommergue, A., and Poulain, A.: The fate of mercury in Arctic terrestrial and aquatic ecosystems, a review, Environ. Chem, 9, 321–355, doi:http://dx.doi.org/10.1071/en11140, 2012.

Ebinghaus, R., Kock, H. H., Coggins, A. M., Spain, T. G., Jennings, S. G., and Temme, C.: Long-term measurements of atmospheric mercury at Mace Head, Irish west coast, between 1995 and 2001, Atmospheric Environment, 36, 5267 – 5276, 2002.

Ebinghaus, R., Jennings, S., Kock, H., Derwent, R., Manning, A., and Spain, T.: Decreasing trends in total gaseous mercury observations in baseline air at Mace Head, Ireland from 1996 to 2009, Atmospheric Environment, 45, 3475 – 3480, 2011.

Feng, X., Shang, L., Wang, S., Tang, S., and Zheng, W.: Temporal variation of total gaseous mercury in the air of Guiyang, China, Journal Of Geophysical Research - Atmospheres, 109, –, 2004.

Fisher, J., Jacob, D., and Sunderland, A. S. H. A. A. S. E.: Riverine source of Arctic Ocean mercury inferred from atmospheric observations, NATURE GEOSCIENCE, 5, 499–504, doi:10.1038/NGEO1478, 2012.

Fu, X., Feng, X., Zhu, W., Wang, S., and Lu, J.: Total gaseous mercury concentrations in ambient air in the eastern slope of Mt. Gongga, South-Eastern fringe of the Tibetan plateau, China, Atmospheric Environment, 42, 970 – 979, 2008a.

Fu, X., Feng, X., Zhu, W., Zheng, W., Wang, S., and Lu, J. Y.: Total particulate and reactive gaseous mercury in ambient air on the eastern slope of the Mt. Gongga area, China, Applied Geochemistry, 23, 408 – 418, 2008b.

Fu, X., Feng, X., Dong, Z., Yin, R., Wang, J., Yang, Z., and Zhang, H.: Atmospheric gaseous elemental mercury (GEM) concentrations and mercury depositions at a high-altitude mountain peak in south China, Atmospheric Chemistry and Physics, 10, 2425 – 2437, 2010.

Fu, X., Feng, X., Liang, P., amd H Zhang, D., Ji, J., and Liu, P.: Temporal trend and sources of speciated atmospheric mercury at Waliguan GAW station, Northwestern China, Atmospheric Chemistry and Physics, 12, 1951 – 1964, 2012a.

Fu, X., Feng, X., Shang, L., Wang, S., and Zhang, H.: Two years of measurements of atmospheric total gaseous mercury (TGM) at a remote site in Mt. Changbai area, Northeastern China, Atmospheric Chemistry and Physics, 12, 4215 – 4226, 2012b.

Fu, X., Zhang, H., Yu, B., Wang, X., Lin, C., and Feng, X.: Observations of atmospheric mercury in China: a critical review, Atmospheric Chemistry and Physics, 15, 9455–9476, doi:10.5194/acp-15-9455-2015, 2015.

Gay, D., Schmeltz, D., Prestbo, E., Olson, M., Sharac, T., and Tordon, R.: The atmospheric mercury network: measurement and initial examination of an ongoing atmospheric mercury record across North America, Atmospheric Chemistry and Physics, 13, 10 521–10 546, 2013.

Gencarelli, C., Simone, F. D., Hedgecock, I., Sprovieri, F., Yang, X., and Pirrone, N.: European and Mediterranean mercury modelling: Local and long-range contributions to the deposition flux, Atmospheric environment Pergamon., 117, 162–168, doi:10.1016/j.atmosenv.2015.07.015, 2015.

Gencarelli, C. N., Bieser, J., Carbone, F., De Simone, F., Hedgecock, I. M., Matthias, V., Travnikov, O., Yang, X., and Pirrone, N.: Sensitivity model study of regional mercury dispersion in the atmosphere, Atmospheric Chemistry and Physics Discussions, 2016, 1–24, doi:10.5194/acp-2016-663, http://www.atmos-chem-phys-discuss.net/acp-2016-663/, 2016.

Goodsite, M., Plane, J., and Skov, H.: A theoretical study of the oxidation of Hg-0 to HgBr2 in the troposphere, Environmental Science & Technology, 38, 1772–1776, doi:10.1021/es034680s, 2004.

Goodsite, M., Plane, J., and Skov, H.: Correction to a theoretical study of the oxidation of Hg0 to HgBr2 in the troposphere, Environmental Science & Technology, 46, 5262–5262, doi:10.1021/es301201c, 2012.

Gustin, M., Amos, H., Huang, J., Miller, M., and Heidecorn, K.: Measuring and modeling mercury in the atmosphere: a critical review, Atmospheric Chemistry and Physics, 15, 5697–5713, doi:10.5194/acp-15-5697-2015, 2015.

Hedgecock, I. and Pirrone, N.: Modelling chemical and physical processes of Hg compounds in the marine boundary layer. In: Dynamics of Mercury Pollution on Regional and Global Scales, N. Pirrone and K. Mahaffey (Editors), Springer Verlag Publishers, Norwell, 2005.

Hedgecock, I. M. and Pirrone, N.: Chasing Quicksilver: Modeling the Atmospheric Lifetime of Hg0(g) in the Marine Boundary Layer at Various Latitudes, Environmental Science & Technology, 38, 69–76, 2004.

Hedgecock, I. M., Pirrone, N., Trunfio, G. A., and Sprovieri, F.: Integrated mercury cycling, transport, and air-water exchange (MECAWEx) model, Journal Of Geophysical Research - Atmospheres, 111, D20 302–, 2006.

Hedgecock, I. M., Pirrone, N., and Sprovieri, F.: Chasing quicksilver northward: mercury chemistry in the Arctic troposphere, Environmental Chemistry, 5, 131–134, 2008.

Higueras, P., Oyarzun, R., Kotnik, J., Esbrí, J., amd M. Horvat, A. M.-C., López-Berdonces, M., Llanos, W., Vaselli, O., Nisi, B., Mashyanov, N., Ryzov, V., Spiric, Z., Panichev, N., McCrindle, R., Feng, X., Fu, X., Lillo, J., Loredo, J., García, M., Alfonso, P., Villegas, K., Palacios, S., Oyarzún, J., Maturana, H., Contreras, F., Adams, M., Ribeiro-Guevara, S., Niecenski, L., Giammanco, S., and Huremović, J.: A compilation of field surveys on gaseous elemental mercury (GEM) from contrasting environmental settings in Europe, South America, South Africa and China: separating fads from facts, Environ Geochem Health, 36, 713–34, doi:10.1007/s10653-013-9591-2, 2014.

Holmes, C. D., Jacob, D. J., Mason, R. P., and Jaffe, D. A.: Sources and deposition of reactive gaseous mercury in the marine atmosphere, Atmospheric Environment, 43, 2278 – 2285, 2009.

Hynes, A. J., Donohoue, D. L., Goodsite, M. E., and Hedgecock, I. M.: Our current understanding of major chemical and physical processes affecting mercury dynamics in the atmosphere and at the air-water/terrestrial interfaces, in: Mercury Fate and Transport in the Global Atmosphere: Emissions, Measurements and Models, edited by Pirrone, N. and Mason, R. P., chap. 14, pp. 427–457, Springer, 2009.

Karunasagar, D., Krishna, M. B., Anjaneyalu, Y., and Arunachalam, J.: Studies of mercury pollution in a lake due to a thermometer factory situated in a tourist resort; Kodaikanal, India.Environmental Pollution, 143, 153–158, 2006.

Kock, H., Bieber, E., Ebinghaus, R., Spain, T., and Thees, B.: Comparison of long-term trends and seasonal variations of atmospheric mercury concentrations at the two European coastal monitoring stations Mace Head, Ireland, and Zingst, Germany, Atmospheric Environment, 39, 7549 – 7556, 2005.

Krishnamoorthya, K. and Mathewb, T.: Inferences on the means of lognormal distributions using generalized p-values and generalized confidence intervals, Journal of Statistical Planning and Inferenc, 115, 103–121, doi:10.1016/S0378-3758(02)00153-2, 2003.

Kurokawa, J., Ohara, T., Morikawa, T., Hanayama, S., Janssens-Maenhout, G., Fukui, T., Kawashima, K., and Akimoto, H.: Emissions of air pollutants and greenhouse gases over Asian regions during 2000- 2008: Regional Emission inventory in ASia (REAS) version 2, Atmos. Chem. Phys., 13, 11 019–11 058, doi:10.5194/acp-13-11019-2013, 2013.

Lacerda, L., de Souzab, M., and Ribeiro, M.: The effects of land use change on mercury distribution in soils of Alta Floresta, Southern Amazon, Environmental Pollution, 129, 247–255, 2004.

Landis, M., Stevens, R., Schaedlich, F., and Prestbo, E.: Development and characterization of an annular denuder methodology for the measurement of divalent inorganic reactive gaseous mercury in ambient air, Environmental Science & Technology, 36, 3000–3009, doi:10.1021/es015887t, 2002.

Lin, C., Pan, L., Streets, D., Shetty, S., Jang, C., Feng, X., and Ho, H. C. T.: Estimating mercury emission outflow from East Asia using CMAQ-Hg, Atmos. Chem. Phys., 10, 1853–1864, doi:10.5194/acp-10-1853-2010, 2010.

Lindberg, S. and Stratton, W.: Atmospheric mercury speciation: concentrations and behavior of reactive gaseous mercury in ambient air, Environmental Science and Technology, 32, 49–57, doi:10.1021/es970546u, 1998.

Lindberg, S., Brooks, S., Lin, C., Scott, K., Landis, M., Stevens, R., and Goodsite, M.: Dynamic oxidation of gaseous mercury in the arctic troposphere at polar sunrise, Environmental Science and Technology, 36, 1245–1256, 2002.

Lindberg, S., Bullock, R., Ebinghaus, R., Engstrom, D., Feng, X., Fitzgerald, W., Pirrone, N., Prestbo, E., and Seigneur, C.: A synthesis of progress and uncertainties in attributing the sources of mercury in deposition, Environmental Science and Technology, 36, 19–33, doi:http://dx.doi.org/10.1579/0044-7447(2007)36[19:ASOPAU]2.0.CO;2, 2007.

Mason, R. P.: Mercury emissions from natural processes and their importance in the global mercury cycle, in: Mercury Fate and Transport in the Global Atmosphere: Emissions, Measurements and Models, edited by Pirrone, N. and Mason, R. P., chap. 7, pp. 173–191, Springer, 2009.

Mendes, N. L. S.: Total Gaseous Mercury (TGM) measurements at the Cape Verde Atmospheric Observatory (CVAO), Tech. rep., University of York, Chemistry (York), http://etheses.whiterose.ac.uk/6616/, 2014.

Mohan, M., Deepa, M., Ramasamy, E., and Thomas, A.: Accumulation of mercury and other heavy metals in edible fishes of Cochin backwaters, Southwest India. Environ Monit Assess, Atmos. Chem. Phys., 184, 4233–4245, doi:10.1007/s10661-011-2258-5, 2012.

Mukherjee, A., Bhattacharya, P., Sarkar, A., and Zevenhoven, R.: Mercury emissions from industrial sources in India. In: Mercury Fate and Transport in the Global Atmosphere: Measurements, models and policy implications (Pirrone N. and Mason R. Eds.), UNEP, 2008.

Muller, D., Wip, D., Warneke, T., Holmes, C., Dastoor, A., and Notholt, J.: Sources of atmospheric mercury in the tropics: continuous observations at a coastal site in Suriname, Atmospheric Chemistry and Physics, 12, 7391–7397, 2012.

Munthe, J., Wängberg, I., Pirrone, N., Iverfeldt, A., Ferrara, R., Ebinghaus, R., Feng, X., Gårdfeldt, K., Keeler, G., Lanzillotta, E., Lindberg, S. E., Lu, J., Mamane, Y., Prestbo, E., Schmolke, S., Schroeder, W. H., Sommar, J., Sprovieri, F., Stevens, R. K., Stratton, W., Tuncel, G., and Urba, A.: Intercomparison of methods for sampling and analysis of atmospheric mercury species, Atmospheric Environment, 35, 3007 – 3017, 2001.

Munthe, J., Wängberg, I., Iverfeldt, A., Lindqvist, O., Stomberg, D., Sommar, J., Gårdfeldt, K., Petersen, G., Ebinghaus, R., Prestbo, E., Larjava, K., and Siemens, V.: Distribution of atmospheric mercury species in Northern Europe: final results from the MOE project, Atmospheric Environment, 37, 9 – 20, 2003.

Munthe, J., Sprovieri, F., Horvat, M., and Ebinghaus, R.: SOPs and QA/QC protocols regarding measurements of TGM, GEM, RGM, TPM and mercury in precipitation in cooperation with WP3, WP4 and WP5, GMOS deliverable 6.1, CNR-IIA, IVL, 2011.

Nguyen, Q., Skov, H., Sørensen, L., Jensen, B., Grube, A., Massling, A., Glasius, M., and Nøjgaard, J.: Source apportionment of particles at Station Nord, North East Greenland during 2008–2010 using COPREM and PMF analysis, Atmos. Chem. Phys., 13, 35–49, 2013.

Pacyna, E., Pacyna, J., Sundseth, K., Munthe, J., Kindbom, K., Wilson, S., Steenhuisen, F., and Maxson, P.: Global emission of mercury to the atmosphere from anthropogenic sources in 2005 and projections to 2020, Atmos. Environ., 44, 2487–2499, doi:10.1016/j.atmosenv.2009.06.009, 2010.

Penney, K. and Cronshaw, I.: Coal in India 2015, Tech. rep., Australian Government - Department of Industry and Science, http://www.chem.unep.ch/mercury/Sector-Specific-Information/FateandTransport(1).htm, 2015.

Pfaffhuber, K., Berg, T., Hirdman, D., and Stohl, A.: Atmospheric mercury observations from Antarctica: seasonal variation and source and sink region calculations, Atmospheric Chemistry and Physics, 12, 3241–3251, doi:10.5194/acp-12-3241-2012, 2012.

Pirrone, N.: GMOS DATA POLICY, http://www.gmos.eu/public/GMOS-Governance_Data_Policy_rev160705.pdf, 2012.

Pirrone, N.: Atmospheric mercury at High Altitude sites: transport patterns and emission source regions, In preparation, Special Issue: Global Mercury Observation System – Atmosphere (GMOS-A), 2016.

Pirrone, N., Ferrara, R., Hedgecock, I., Kallos, G., Mamane, Y., Munthe, J., Pacyna, J., Pytharoulis, I., Sprovieri, F., Voudouri, A., and Wängberg, I.: Dynamic Processes of Mercury Over the Mediterranean Region: results from the Mediterranean Atmospheric Mercury Cycle System (MAMCS) project, Atmospheric Environment, 37, 21–39, doi:10.1016/S1352-2310(03)00251-6, 2003.

Pirrone, N., Hedgecock, I., and Sprovieri, F.: Atmospheric mercury, easy to spot and hard to pin down: impasse?, Atmospheric Environment, 42, 8549–8551, doi:10.1016/j.atmosenv.2008.09.004, 2008.

Pirrone, N., Cinnirella, S., Feng, X., Finkelman, R., Friedli, H., Leaner, J., Mason, R., Mukherjee, A., Stracher, G., Streets, D., and Telmer, K.: Global mercury emissions to the atmosphere from natural and anthropogenic sources, in: Mercury Fate and Transport in the Global Atmosphere: Emissions, Measurements, and Models, edited by Pirrone, N. and Mason, R., pp. 3–49, Springer, 2009.

Pirrone, N., Cinnirella, S., Feng, X., Finkelman, R., Friedli, H., Leaner, J., Mason, R., Mukherjee, A., Stracher, G., Streets, D., and Telmer, K.: Global mercury emissions to the atmosphere from anthropogenic and natural sources, Atmos. Chem. Phys, 10, 5951–5964, doi:10.5194/acp-10-5951-2010, 2010.

Pirrone, N., Aas, W., Cinnirella, S., Ebinghaus, R., Hedgecock, I., Pacyna, J., Sprovieri, F., and Sunderland, E.: Toward the next generation of air quality monitoring: Mercury, Atmospheric Environment, 80, 599–611, doi:10.1016/j.atmosenv.2013.06.053, 2013.

Poulain, A., Lalonde, J., Amyot, M., Shead, J., Raofie, F., and Ariya, P.: Redox transformations of mercury in an Arctic snowpack at springtime, Atmospheric Environment, 38, 6763–6774, doi:10.1016/j.atmosenv.2004.09.013, 2004.

Rajgopal, T. and Mascarenhas, H. R. P.: Epidemiologicalsurveillance of employees in a mercury thermometer plant: An occupational health study, Indian J. Occup. and Environ. Med., 10, 11–18, 2006.

Selin, N. E., Jacob, D. J., Yantosca, R. M., Strode, S., Jaeglé, L., and Sunderland, E. M.: Global 3-D land-ocean-atmosphere model for mercury: Present-day versus preindustrial cycles and anthropogenic enrichment factors for deposition, Global Biogeochem. Cycles, 22, GB2011, 2008.

Sena, F., Umlauf, G., Ruiz, A. A., Islas, M. R., Trejo, J. A. V., Cabrera, F. A., and Vargas, I. O.: Wet deposition and atmospheric mercury monitoring in Sisal, Yucatán, México, as part of the Global Mercury Observation System (GMOS), Tech. rep., JRC - EUROPEAN COMMISION, doi:10.2788/823558, 2015.

Sheu, G., Lin, N., Lee, C., Wang, J., Chuang, M., Wang, S., Chi, K., and Ou-Yang, C.: Distribution of atmospheric mercury in northern Southeast Asia and South China Sea during Dongsha Experiment, Atmospheric Environment, 78, 174–183, doi:doi:10.1016/j.atmosenv.2012.07.002, 2013.

Sholupov, S. and Ganeyev, A.: Zeeman atomic absorption spectrometry using high frequency modulated light polarization, Spectrochimica Acta Part B: Atomic Spectroscopy, 50, 1227–1236, doi:10.1016/0584-8547(95)01316-7, 1995.

Sholupov, S., Pogarev, S., Ryzhov, V., Mashyanov, N., and Stroganov, A.: Zeeman atomic absorption spectrometer RA-915+ for direct determination of mercury in air and complex matrix samples, Fuel Processing Technology, 85, 473–485, doi:10.1016/j.fuproc.2003.11.003, 2004.

Skov, H., Christensen, J. H., Goodsite, M. E., Heidam, N. Z., Jensen, B., Wåhlin, P., and Geernaert, G.: Fate of Elemental Mercury in the Arctic during Atmospheric Mercury Depletion Episodes and the Load of Atmospheric Mercury to the Arctic, Environmental Science & Technology, 38, 2373–2382, 2004.

Skov, H., Goodsite, M., Lindberg, S., Meyers, T., Landis, M., Larsen, M., and McConville, G.: The fluxes of Reactive Gaseous mercury measured with a newly developed method using relaxed eddy accumulation, Atmospheric Environment, 40, 5452–5463, doi:10.1016/j.atmosenv.2006.04.061, 2006.

Slemr, F., Brunke, E.-G., Ebinghaus, R., and Kuss, J.: Worldwide trend of atmospheric mercury since 1995, Atmospheric Chemistry and Physics, 11, 4779–4787, doi:10.5194/acp-11-4779-2011, 2011.

Slemr, F., Angot, H., Dommergue, A., Magand, O., Barret, M., Weigelt, A., Ebinghaus, R., Brunke, E.-G., Pfaffhuber, K., Edwards, G., abd J. Powell, D. H., Keywood, M., and Wang, F.: Comparison of mercury concentrations measured at several sites in the Southern Hemisphere, Atmospheric Chemistry and Physics, 15, 3125–3133, doi:10.5194/acp-15-3125-2015, 2015.

Soerensen, A., Skov, H., Soerensen, D. J. B., and Johnson, M.: Global concentrations of gaseous elemental mercury and reactive gaseous mercury in the marine boundary layer, Environmental Science and Technology, 44, 7425–7430, doi:10.1021/es903839n, 2010a.

Soerensen, A., Sunderland, E., Holmes, C., Jacob, D., Yantosca, R., Skov, H., Christensen, J., Strode, S., and Mason, R.: An improved global model for air-sea exchange of mercury: high concentrations over the North Atlantic, Environmental Science and Technology, 44, 8574–8580, doi:10.1021/es102032g, 2010b.

Sommar, J., Andersson, M. E., and Jacobi, H.-W.: Circumpolar measurements of speciated mercury, ozone and carbon monoxide in the boundary layer of the Arctic Ocean, Atmospheric Chemistry and Physics, 10, 5031–5045, 2010.

Sprovieri, F., Pirrone, N., Hedgecock, I., Landis, M., and Stevens, R.: Intensive atmospheric mercury measurements at Terra Nova Bay in antarctica during November and December 2000, Journal of geophysical research, 107, ACH 20–1–ACH 20–8, doi:10.1029/2002JD002057, 2002.

Sprovieri, F., Pirrone, N., Landis, M., and Stevens, R.: Oxidation of gaseous elemental mercury to gaseous divalent mercury during 2003 polar sunrise at Ny-Alesund, Environmental Science and Technology, 39, 9156–9165, doi:10.1021/es050965o, 2005a.

Sprovieri, F., Pirrone, N., Landis, M., and Stevens, R.: Atmospheric mercury behaviour at different altitudes at NyAlesund during Spring 2003, Atmospheric Chemistry and Physics, 39, 7646–7656, doi:10.1016/j.atmosenv.2005.08.001, 2005b.

Sprovieri, F., Hedgecock, I., and N., P.: An Investigation of the origins of reactive gaseous mercury in the Mediterranean marine boundary layer, Atmospheric Chemistry and Physics, 10, 3985–3997, doi:10.5194/acp-10-3985-2010, 2010a.

Sprovieri, F., Pirrone, N., Ebinghaus, R., and Kock, H.: A review of worldwide atmospheric mercury measurements, Atmospheric Chemistry and Physics, 10, 8245–8265, doi:10.5194/acp-10-8245-2010, 2010b.

Sprovieri, F., Gratz, L., and Pirrone, N.: Development of a ground based atmospheric monitoring network for the Global Mercury Observation System (GMOS)., in: E3S web Conference, doi:10.1051/e3sconf/20130117007, 2013.

Sprovieri, F., Pirrone, N., Bencardino, M., D'Amore, F., Angot, H., Barbante, C., Brunke, E.-G., Arcega-Cabrera, F., Cairns, W., Comero, S., Diéguez, M. D. C., Dommergue, A., Ebinghaus, R., Feng, X. B., Fu, X., Garcia, P. E., Gawlik, B. M., Hageström, U., Hansson, K., Horvat, M., Kotnik, J., Labuschagne, C., Magand, O., Martin, L., Mashyanov, N., Mkololo, T., Munthe, J., Obolkin, V., Islas, M. R., Sena, F., Somerset, V., Spandow, P., Vardè, M., Walters, C., Wängberg, I., Weigelt, A., Yang, X., and Zhang, H.: Five-year records of Total Mercury Deposition flux at GMOS sites in the Northern and Southern Hemispheres, Atmospheric Chemistry and Physics Discussions, 2016, 1–33, doi:10.5194/acp-2016-517, http://www.atmos-chem-phys-discuss.net/acp-2016-517/, 2016.

Steffen, A., Douglas, T., Amyot, M., Ariya, P., Aspmo, K., Berg, T., Bottenheim, J., Brooks, S., Cobbett, F., Dastoor, A., Dommergue, A., Ebinghaus, R., Ferrari, C., Gardfeldt, K., Goodsite, M., Lean, D., Poulain, A., Scherz, C., Skov, H., Sommar, J., and Temme, C.: A synthesis of atmospheric mercury depletion event chemistry in the atmosphere and snow, Atmospheric Chemistry and Physics, 8, 1445–1482, doi:10.5194/acp-8-1445-2008, 2008.

Steffen, A., Scherz, T., Olson, M., Gay, D., and Blanchard, P.: A comparison of data quality control protocols for atmospheric mercury speciation measurements, Journal of Environmental Monitoring, 14, 752–765, 2012.

Streets, D. G., Hao, J., Wu, Y., Jiang, J., Chan, M., Tian, H., and Feng, X.: Anthropogenic mercury emissions in China, Atmospheric Environment, 39, 7789 – 7806, 2005.

Streets, D. G., Devane, M. K., Lu, Z., Bond, T. C., Sunderland, E. M., and Jacob, D. J.: All-Time Releases of Mercury to the Atmosphere from Human Activities, Environmental Science & Technology, 45, 10 485 – 10 491, 2011.

Subir, M., Ariya, P. A., and Dastoor, A. P.: A review of uncertainties in atmospheric modeling of mercury chemistry I. Uncertainties in existing kinetic parameters–Fundamental limitations and the importance of heterogeneous chemistry., Atmospheric Environment, 45.32, 5664–5676, 2011.

Subir, M., Ariya, P. A., and Dastoor, A. P.: A review of the sources of uncertainties in atmospheric mercury modeling II. Mercury surface and heterogeneous chemistry – A missing link, Atmospheric Environment, 46, 1 – 10, 2012.

Temme, C., Einax, J. W., Ebinghaus, R., and Schroeder, W. H.: Measurements of Atmospheric Mercury Species at a Coastal Site in the Antarctic and over the South Atlantic Ocean during Polar Summer, Environmental Science & Technology, 37, 22–31, 2003.

Temme, C., Blanchard, P., Steffen, A., Banic, C., Beauchamp, S., Poissant, L., Tordon, R., and Wiens, B.: Trend, seasonal and multivariate analysis study of total gaseous mercury data from the Canadian atmospheric mercury measurement network (CAMNet), Atmospheric Environment, 41, 5423 – 5441, 2007.

UNEP: UNEP: Mercury fate and transport in the global atmosphere: Measurements, models and policy implications, Tech. rep., UNEP Global Mercury Partnership Mercury Air Transport and Fate Research partnership area, http://www.chem.unep.ch/mercury/Sector-Specific-Information/FateandTransport(1).htm, 2008.

van Donkelaar, A., Martin, R., Brauer, M., Kahn, R., Levy, R., and Verduzco, C.: Global estimates of ambient fine particulate matter concentrations from satellite-based aerosol optical depth: development and application, Environ Health Perspect, 118, 847–855, doi:10.1289/ehp.0901623., 2010.

Wang, Z., Zhang, X., Chen, Z., and Zhang, Y.: Mercury concentrations in size-fractionated airborne particles at urban and suburban sites in Beijing, Atmospheric Environment, 40, 2194–2201, doi:10.1016/j.atmosenv.2005.12.003, 2006.

Wang, Z., Chen, Z., Duan, N., and Zhang, X.: Gaseous elemental mercury concentration in atmosphere at urban and remote sites in China, J. Environ. Sci., 19, 176–180, doi:10.1016/S1001-0742(07)60028-X, 2007.

Wängberg, I., Munthe, J., Pirrone, N., Iverfeldt, A., Bahlman, E., Costa, P., Ebinghaus, R., Feng, X., Ferrara, R., Gardfeldt, K., Kock, H., Lanzillotta, E., Mamane, Y., Mas, F., Melamed, E., Osnat, Y., Prestbo, E., Sommar, J., Schmolke, S., Spain, G., Sprovieri, F., and Tuncel, G.: Atmospheric mercury distribution in Northern Europe and in the Mediterranean region, Atmospheric Environment, 35, 3019 – 3025, 2001.

Wängberg, I., Munthe, J., Amouroux, D., Andersson, M., Fajon, V., Ferrara, R., Gårdfeldt, K., Horvat, M., Mamane, Y., Melamed, E., Monperrus, M., Ogrinc, N., Yossef, O., Pirrone, N., Sommar, J., and Sprovieri, F.: Atmospheric mercury at mediterranean coastal stations, Environmental Fluid Mechanics, 8, 101–116, 2008.

Weigelt, A., Ebinghaus, R., Manning, A., Derwent, R., Simmonds, P., Spain, T., Jennings, S., and Slemr, F.: Analysis and interpretation of 18 years of mercury observations since 1996 at Mace Head, Ireland, Atmospheric Environment, 100, 85–93, doi:10.1016/j.atmosenv.2014.10.050, 2015.

Weigelt, A., Ebinghaus, R., Pirrone, N., Bieser, J., Bödewadt, J., Esposito, G., Slemr, F., van Velthoven, P. F. J., Zahn, A., and Ziereis, H.: Tropospheric mercury vertical profiles between 500 and 10â€¯000 m in central Europe, Atmospheric Chemistry and Physics, 16, 4135–4146, doi:10.5194/acp-16-4135-2016, http://www.atmos-chem-phys.net/16/4135/2016/, 2016.

Wu, Y., Wang, S., Streets, D. G., Hao, J., Chan, M., and Jiang, J.: Trends in Anthropogenic Mercury Emissions in China from 1995 to 2003, Environmental Science & Technology, 40, 5312–5318, 2006.

Xiu, G., Cai, J., Zhang, W., Zhang, D., Bueler, A., Lee, S., Shen, Y., Xu, L., Huang, X., and Zhang, P.: Speciated mercury in size-fractionated particles in Shanghai ambient air, Atmos. Environ., 43, 3145–3154, doi:10.1016/j.atmosenv.2008.07.044, 2009.

Xu, L., Chen, J., Yang, L., Niu, Z., Tong, L., Yin, L., and Chen, Y.: Characteristics and sources of atmospheric mercury speciation in a coastal city, Xiamen, China, Chemosphere, 119, 530–539, doi:10.1016/j.chemosphere.2014.07.024, 2015.

Zhang, H., Fu, X., Lin, C., Wang, X., Feng, X., Yu, B., Zhou, J., and Zhang, Y.: Impacts of Indian summer monsoon on distribution of atmospheric mercury at a high-altitude background station, southwestern China, under preparation, 2015.

Zhang, L., Wang, S., and Hao, J.: Atmospheric mercury concentration and chemical speciation at a rural site in Beijing, China: implications of mercury emission sources, Atmospheric Chemistry and Physics, 13, 10 505–10 516, doi:10.5194/acp-13-10505-2013, 2013.

Zhu, J., Wang, T., Talbot, R., Mao, H., Yang, X., Fu, C., Sun, J., Zhuang, B., Li, S., Han, Y., and Xie, M.: Characteristics of atmospheric mercury deposition and size-fractionated particulate mercury in urban Nanjing, China, Atmos. Chem. Phys., 14, 2233–2244, doi:10.5194/acp-14-2233-2014, 2014.